


Global spatiotemporal optimization of photovoltaic and wind power to achieve the Paris Agreement targets

Received: 23 January 2024

Accepted: 14 February 2025

Published online: 03 March 2025

 Check for updates

Yijing Wang¹, Rong Wang ^{1,2,3,4,5,6,7} ✉, Katsumasa Tanaka ^{8,9}, Philippe Ciais ^{8,10}, Josep Penuelas ^{11,12}, Yves Balkanski ⁸, Jordi Sardans ^{11,12}, Didier Hauglustaine ⁸, Junji Cao¹³, Jianmin Chen ^{1,2,3}, Lin Wang ^{1,2,3}, Xu Tang^{2,3} & Renhe Zhang ^{2,3,4}

Limiting global warming below 1.5 or 2 °C calls for achieving energy systems with net-zero carbon dioxide (CO₂) emissions likely by 2040 or 2070, but the pledged actions under current policies cannot meet these targets. Few studies have optimized global deployment of photovoltaic and wind power. Here we present a strategy involving construction of 22,821 photovoltaic, onshore-wind, and offshore-wind plants in 192 countries worldwide to minimize the levelized cost of electricity. We identify a large potential of cost reduction by combining coordination of energy storage and power transmission, dynamics of learning, trade of minerals, and development of supply chains. Our optimization increases the capacity of photovoltaic and wind power, accompanied by a reduction in the average cost of abatement from US Dollars (\$) 140 (baseline) to \$33 per tonne CO₂. Our study provides a global roadmap for achieving energy systems with net-zero CO₂ emissions, emphasizing the physical, financial, and socioeconomic challenges forward.

Obtaining a high chance to mitigate global warming from 2 to 1.5 °C without overshoot likely requires advancing the time of net-zero CO₂ emissions from 2070 to 2040^{1,2}, which reduces adverse effects of climate change on economic growth³ with a diminishing risk of irreversible tipping points⁴. This is consistent with the projection that a majority of the 1.5 °C scenarios assessed by the Intergovernmental Panel on Climate Change (IPCC) result in net-zero CO₂ emissions energy supply systems in the 2040 s, while a sizable fraction of them

achieves this target in the 2030s⁵. Global warming has exceeded 1.2 °C in 2022⁶, 1.45 ± 0.12 °C in 2023⁷, and even 1.55 °C⁸ in 2024 above pre-industrial level, leaving a narrow window to meet the Paris Agreement long-term temperature goal⁹. However, over 90% of the 1.5 °C scenarios assessed by IPCC rely on deploying large-scale negative emission technologies such as carbon capture and storage (CCS), afforestation, and soil carbon sequestration to sequester 2–10 Giga tonne carbon dioxide per year (Gt CO₂ y⁻¹) by 2050, and up to 15–20 Gt

¹Shanghai Key Laboratory of Atmospheric Particle Pollution and Prevention (LAP³), Department of Environmental Science and Engineering, Fudan University, Shanghai, China. ²IRDR International Center of Excellence on Risk Interconnectivity and Governance on Weather/Climate Extremes Impact and Public Health, Fudan University, Shanghai, China. ³Institute of Atmospheric Sciences, Fudan University, Shanghai, China. ⁴Shanghai Frontiers Science Center of Atmosphere-Ocean Interaction, Shanghai, China. ⁵MOE Laboratory for National Development and Intelligent Governance, Fudan University, Shanghai, China. ⁶Institute of Eco-Chongming (IEC), Shanghai, China. ⁷National Observations and Research Station for Wetland Ecosystems of the Yangtze Estuary, Fudan University, Shanghai, China. ⁸Laboratoire des Sciences du Climat et de l'Environnement (LSCE), CEA/CNRS/UVSQ, IPSL, Université Paris-Saclay, Gif-sur-Yvette, France. ⁹Earth System Division, National Institute for Environmental Studies (NIES), Tsukuba, Japan. ¹⁰Climate and Atmosphere Research Center (CARE-C) The Cyprus Institute 20 Konstantinou Kavafi Street, Nicosia, Cyprus. ¹¹CSIC, Global Ecology Unit CREAM-CSIC-UAB, Bellaterra, Catalonia, Spain. ¹²CREAF, Cerdanyola del Vallès, Catalonia, Spain. ¹³Institute of Atmospheric Physics, Chinese Academy of Sciences, Beijing, China.

✉ e-mail: rongwang@fudan.edu.cn

CO₂ y⁻¹ by 2100^{5,10,11}. Large amounts of negative emissions may exceed the biophysical and economic limits of the Earth system¹². Over-reliance on untested technologies increases the risk of carbon lock-in from the continuing construction of fossil-fuel infrastructure¹³.

Despite ambitious promises and pledges including net zeros from many countries, global warming has a 66% chance to reach 2.9 °C in 2100 by continuing unconditional Nationally Determined Contributions (NDCs)¹⁴. The 28th United Nations Climate Change Conference (COP28) focused on the first Global Stocktake, where 116 countries had signed the Global Renewable Energy and Energy Efficiency Commitment aiming at tripling the installed capacities of renewable energy from today to 2030¹⁵. According to a meta-analysis of scenarios generated by integrated assessment models developed using different methods, limiting global warming to 1.5 °C needs an expansion of the capacities of photovoltaic (PV) and wind power from 2.4 to 12 ± 5 (mean ± standard) petawatt-hour per year (PWh y⁻¹) during 2020–2030^{16,17}. A study published in 2021¹⁸ predicted that such demand could not be satisfied unless the current growths of renewable energy were radically accelerated in the coming decades. In the absence of empirically grounded constraints on the floor prices of renewable energy and the maximal capacities of power generation with sufficient geospatial details, current projections of energy transitions^{5,10–12,15,18,19} are pessimistic about a rapid penetration of renewable energy dominated by PV and wind by underestimating the benefits from technological innovations²⁰.

When making ambitious targets about phasing out fossil fuels, a spatially explicit method is urgently needed to unlock the maximal capacities of deploying renewable energy^{21,22}. Such methods have so

far been developed mostly at regional scales, e.g., for China²³, Europe²⁴, and the United States of America (USA)²⁵. To represent grid parity, we estimate the levelized cost of electricity (LCOE) as the present value of total costs including initial investment, operation and maintenance (O&M), land acquisition, grid connection, electricity transmission by ultra-high voltage (UHV) lines, and energy storage, which are divided by the power generation over the lifetime of power plants²³. We optimize the location, capacity, and construction period of PV and wind power plants built at the utility scale (>10 megawatt (MW)) for 2021–2070 to minimize LCOE in the power sector when achieving the net-zero target in a specific year (see Fig. 1 for an overview of our model and see **Methods** for the detailed descriptions of the models and algorithms used for the spatiotemporal optimization). We focus on the scenarios achieving the net-zero target in 2040 or 2070 to be consistent with the 1.5 °C or 2 °C target in the Paris Agreement². For example, the path to achieve the 2050 net-zero target should be one between the scenarios of achieving the 2040 and 2070 net-zero targets.

In this work, we seek solutions to the cost-minimizing problem of all power plants by combining geospatial details of solar radiation and wind power resources, efficiencies of energy conversion, suitability of pixels in power generation, requirements on initial investments, coordination of power transmission and energy storage, dynamics of technological improvements in module costs²⁰, trade of minerals²⁶, and regional supply chains of PV panels and wind turbines²⁷. By estimating the LCOE of PV and wind power, we consider that PV and wind power plants would compete with CCS, bioenergy, geothermal, hydro, nuclear, and tidal wave to be cost-effective in mitigation. Our results

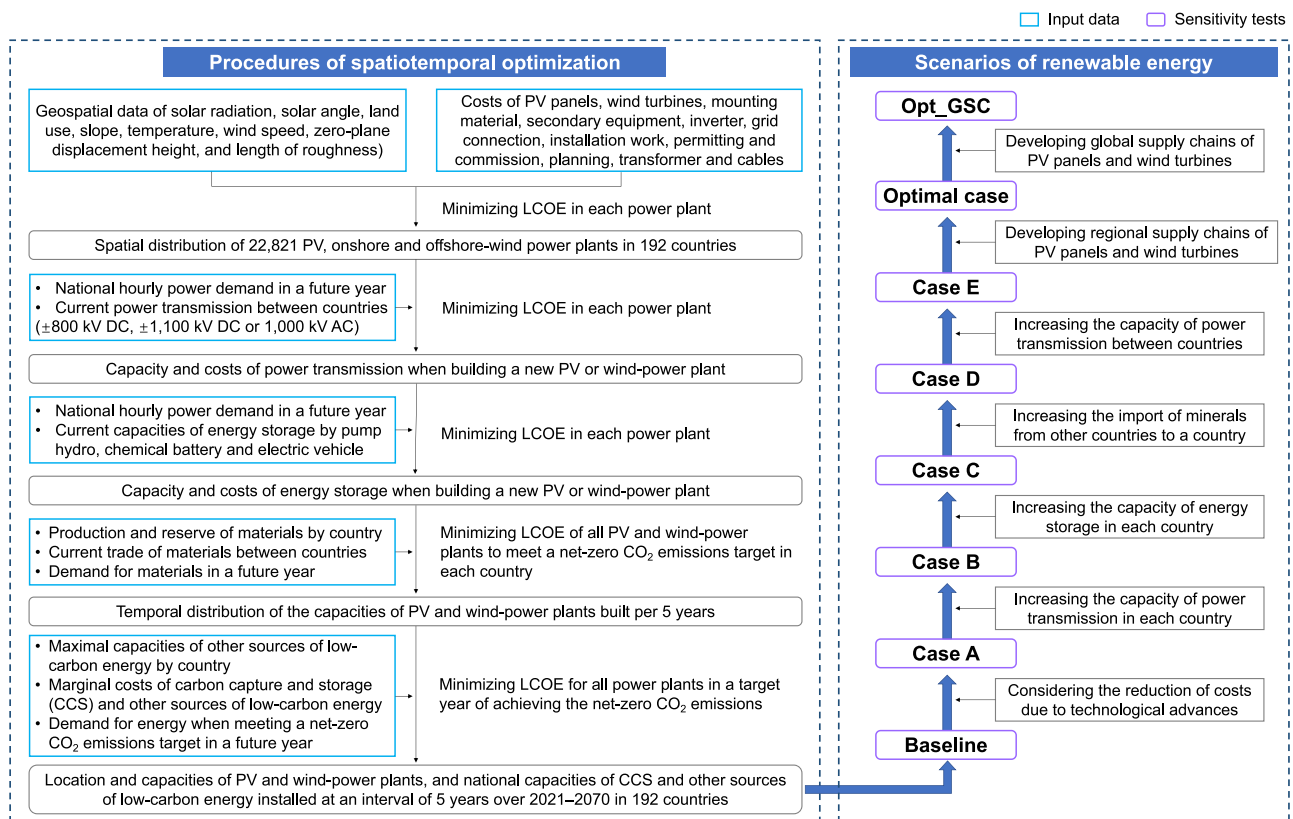


Fig. 1 | An overview of the procedures of spatiotemporal optimization in our model to achieve net-zero CO₂ emissions energy supply systems in 192 countries. Relative to the baseline case based on the current readiness of technologies, we explore seven experiments by considering the effects of technological improvements in cost reduction (Case A), increasing the capacity of domestic power transmission (Case B), increasing the capacity of energy storage (Case C),

increasing the import of minerals from other countries to each country (Case D), increasing the capacity of power transmission between countries (Case E), considering the effects of regional supply chains of PV panels and wind turbines (Optimal case), and considering the effects of global supply chains of PV panels and wind turbines (Opt_GSC case). A detailed description of scenarios is available in Supplementary Table 1.

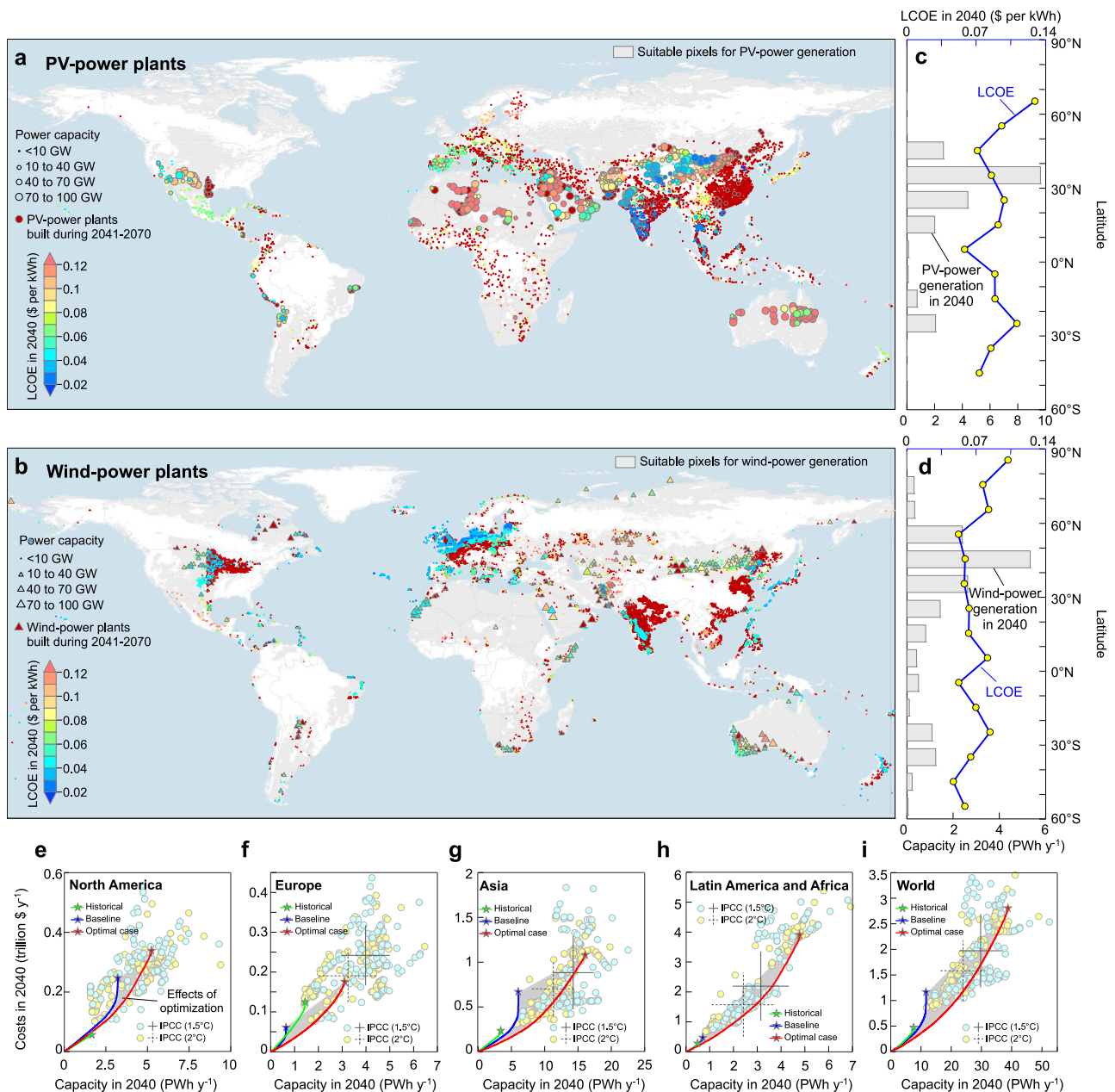


Fig. 2 | Spatiotemporal distribution of photovoltaic (PV) and wind-power plants built to meet the target of achieving net-zero CO₂ emissions energy supply systems by 2040. a, b Geographic distributions of the utility-scale PV (a) and wind (b) power plants built during 2021–2070 when meeting the net-zero target by 2040. The color shows the levelized cost of electricity (LCOE) for the power plants built during 2021–2040. The power plants built after 2040 are shown by the dark red circles or triangles. **c, d** Zonal distributions of the capacities and LCOE of PV (c) and wind (d) power plants in 2040. **e–i** Capacity and costs of PV and

wind-power plants in North America (e), Europe (f), Asia (g), Latin America and Africa (h) and all regions (i) in 2040. The shade denotes the difference between the baseline case and the optimal case. We consider a “Historical” scenario, which keeps the rate of deploying PV and wind power during 2011–2020 unchanged over the period of 2021–2070 (see the text). The yellow and blue circles denote the projected power generation and costs in the IPCC scenarios meeting the 2 °C or 1.5 °C target¹⁶. The crosses denote the averages. Source data are provided as a Source Data file.

demonstrate that it’s technically possible to achieve the net-zero target by 2040, but it requires overcoming the physical, financial, and socioeconomic barriers to accelerate global deployment of PV and wind power.

Results

Global distributions of photovoltaic and wind power plants

When achieving the net-zero target by 2040 in our optimal case, global total power generation by PV, onshore wind, and offshore wind will reach 21.7, 14.7, and 2.3 PWh yr⁻¹ in 2040, with an average LCOE of

\$0.091, \$0.064 and \$0.05 per kWh (all currency values throughout the paper are in 2020 US dollars), respectively (Fig. 2a, b). We notice that the LCOE is predicted to be \$0.048 per kWh for PV power and \$0.033 per kWh for onshore-wind power by the International Renewable Energy Agency²⁸, which do not consider an increase in the marginal abatement costs due to the rising power demand¹⁸. We then derive the marginal abatement cost (MAC) from the incremental cost of abating one tonne of CO₂ emissions when building a new PV or wind-power plant (see results in the following sections). We find that PV power plants are optimally distributed in South and East Asia at a latitude of

20–40°N with total power generation of 14 PWh y^{-1} and an average LCOE of \$0.089 per kWh by accounting for the spatial distributions of solar radiation, land occupation, clouds, land cover, power demand, and capital costs (Fig. 2c). Wind-power plants are more homogeneously distributed in space (Fig. 2d), due to less requirements of land occupation for wind turbines than for PV panels. Although a fraction of the land area requirement for wind-power plants has permanent, direct impacts on land use^{29,30}, societal acceptance should be considered due to the visual impact when constructing wind turbines at sites that are close to residential areas. We evaluate the accuracy of the spatial distributions of PV and wind-power generation by changing the geospatial data used for land use, solar radiation, wind speed, and air temperature in our model (Supplementary Fig. 1). If the standard data of land use³¹ is replaced with data from a study published in 2024³², the predicted PV and wind-power generation will decrease in the West of the USA, the East of China, Europe, Africa, and South America, but increase over the East of USA and the West of China. If the spatial resolutions of solar radiation, wind speed, and air temperature decrease from $0.5^\circ \times 0.625^\circ$ to $1^\circ \times 1^\circ$, the total PV and wind-power generation will change moderately, but the peak value will decrease.

In our optimal case, the projected cost reduction by technological improvements²⁰ and the low-cost energy sources identification at sub-national scales²³ together lead to a faster growth of PV and wind-power generation than the prediction based on the historical trends. The inclusion of the spatial details of solar radiation and wind speed allows us to provide an empirically grounded estimate of physical constraints on the maximal capacities¹² while representing the hour-to-hour variation of power generation and consumption captures the economic costs due to the rising demand for power transmission and energy storage²⁴. For example, extrapolating the growth rates in the 2010s to the period of 2021–2040¹⁷ with previous estimates of costs³³ leads to global PV and wind power generation of 7.5 PWh y^{-1} with annualized costs of only \$0.44 trillion y^{-1} in 2040 (Fig. 2e–i). This capacity is far below the average of 102 scenarios (29.6 PWh y^{-1}), meeting the 1.5°C target that are assessed by IPCC¹⁶. By contrast, in a baseline case, a large fraction of PV and wind power plants with high LCOE are excluded in competition with CCS and other types of low-carbon energy. We project global PV and wind power generation to be 11.6 PWh y^{-1} in 2040 at a total cost of \$1.2 trillion y^{-1} in the baseline case, compared to 38.6 PWh y^{-1} at a total cost of \$2.8 trillion y^{-1} in our optimal case. The higher capacities of PV and wind power make it possible to meet the ambitious climate targets^{5,10,11}, but the larger costs underscore the economic barriers to acceleration mitigation¹⁸. We analyze the factors contributing to these differences in the following sections.

The marginal abatement costs by deploying photovoltaic and wind power plants

We develop a global model to optimize the construction of PV and wind-power plants to minimize LCOE in each country by considering the impacts of regional power transmission, global trade of minerals, and global supply chains of PV panels and wind turbines (Fig. 1). As a result, our model should be distinguished from the regional models by optimizing the global power grids^{23,34–37}. We estimate the MAC by subtracting the revenue of replacing fossil fuels from the costs of deploying PV and wind power, where the MAC is negative when the former is higher than the latter. In our optimal case, we predict the MAC in 2040 to rise from -\$270 per tCO₂ as a minimum by replacing fossil fuels to \$131 per tCO₂ as a maximum by considering the demand for power transmission, energy storage, and regional supply chains of materials (Fig. 3a, b). In the baseline case, we account for the current capacities of energy storage (0.14, 0.09, and 0.23 terawatt (TW) for hydro pump³⁸, chemical battery³⁹ and electric vehicle⁴⁰ in 2023, respectively), domestic power transmission (e.g., current capacity of UHV line in China is 0.74TW²³) and international power transmission (1.12 PWh in 2020²²) (e.g., for power transmissions between countries

in Europe and between the USA and Canada in North America), and the trade of mineral between countries (e.g., 21.3, 4.6, 12.1, 4.3, 17.5, 8.9, and 0.04 megaton (Mt) for copper, Zinc, Nickel, Silicon, Manganese, Chromium, and Rare earth elements in 2021, respectively⁴¹). Relative to the baseline case, we perform six experiments by considering the effects of technological improvements in cost reduction (Case A), increasing the capacity of domestic power transmission (Case B), increasing the capacity of energy storage (Case C), increasing the import of minerals from other countries to each country (Case D), increasing the capacity of power transmission between countries (Case E), and considering the effects of regional supply chains of PV panels and wind turbines (Optimal case) (see the underlying assumptions for each scenario in Fig. 1 and Supplementary Table 1).

From a global aspect, our results highlight the importance of expanding energy storage and power transmission beyond current levels to maintain grid stability when integrating high shares of variable renewable energy^{23,34,36,37,42}. We estimate that expanding the capacities of energy storage and power transmission can increase the fraction of PV and wind-power generation utilized by the end-use sectors (Supplementary Fig. 2). This expansion could, in turn, reduce the consumption of fossil fuels that occur due to the intermittence of renewable energy when meeting the demand for power. When achieving net-zero CO₂ emissions energy supply systems by 2040, we estimate that 8.6% of global PV and wind-power generation will be discarded if the projected capacity of energy storage by 2040, in our optimal case is reduced by 50% from 12.5 to 6.2 TW. Similarly, 10.8% of PV and wind-power generation will be discarded if the projected capacity of power transmission by 2040, in our optimal case is reduced by 50% from 36.1 to 18 TW.

We predict that global CO₂ emissions abatement by PV and wind power plants in 2040 could reach 8.1 Gt CO₂ y^{-1} in the baseline case, compared to 12.9 Gt CO₂ y^{-1} in Case C and 27.5 Gt CO₂ y^{-1} in our optimal case (Fig. 3c). This is accompanied by a reduction in the average MAC from \$140 per tCO₂ in the baseline case to \$93 per tCO₂ in Case C and \$33 per tCO₂ in our optimal case (Fig. 3d). Our optimization leads to greater contributions by Oceania, the Middle East, Africa and Europe to global CO₂ emissions reduction when building more PV and wind power plants from baseline to optimal case. Meanwhile, the contribution of fixed cost, transformers, cable, land, connection to UHV stations, and O&M to total costs decreases from 99 to 63%. The contribution of the costs of energy storage and power transmission to total costs increases from 17 to 37% when achieving the net-zero CO₂ target by 2040 rather than 2070, mainly due to an increase in the demand for low-carbon energy supply (Supplementary Fig. 3). Meanwhile, the contribution of the costs of power transmission and energy storage to total costs varies from 15% in Europe to 46% in Asia when achieving the net-zero target by 2040, mainly due to differences in the demand for low-carbon energy supply across regions. By estimating the global MAC curve of PV and wind power based on dynamics of technological improvements²⁰, our study indicates a cost-minimizing path to increase the capacity of global renewable energy during 2021–2040 as pledged by COP28¹⁵ by accelerating the expansion of PV and wind power.

Comparison of deployment rates among various pathways of emissions

We evaluate the technological readiness levels by comparing the proposed capacities of PV power, onshore and offshore wind power, energy storage, and power transmission by UHV lines in our optimal case with the predicted capacities based on the historical trends^{38–40}, as well as the projections from previous studies^{40,43–51} (Fig. 4). In our central case, we optimize the sequence of constructing power plants over time to minimize the LCOE of all newly built power plants in the target year, either 2040 or 2070. Since the effect of learning depends on the increase in cumulative capacity, more affordable power plants

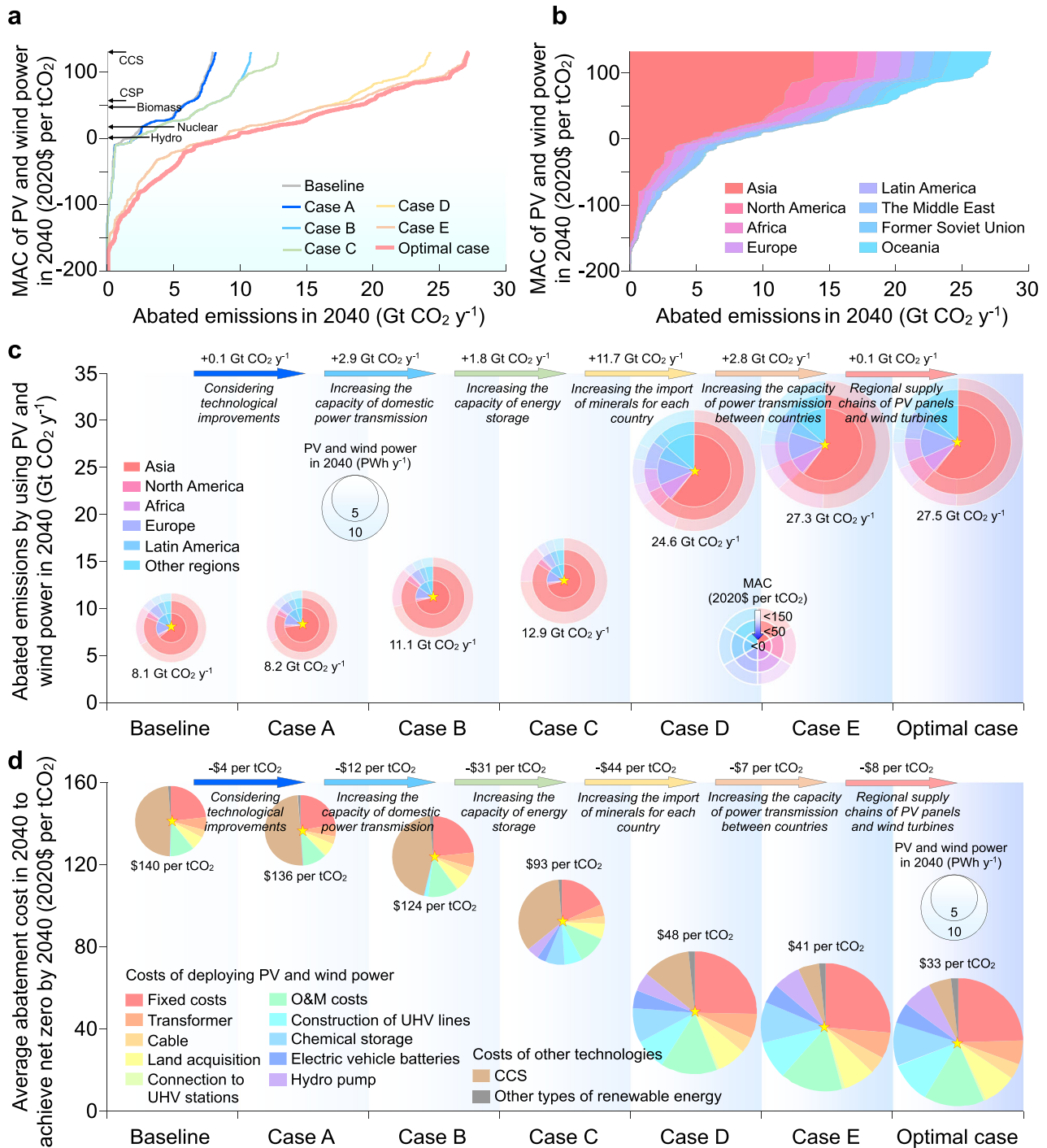


Fig. 3 | Abatement of CO₂ emissions by building new photovoltaic (PV) and wind power plants when achieving energy supply systems with net-zero CO₂ emissions by 2040. a Marginal abatement cost (MAC) of PV and wind power at a plant level during 2021–2040. Relative to the baseline case, we explore six experiments by considering the effects of technological improvements in cost reduction (Case A), increasing the capacity of domestic power transmission (Case B), increasing the capacity of energy storage (Case C), increasing the import of minerals from other countries to each country (Case D), increasing the capacity of power transmission between countries (Case E), and considering the effects of regional supply chains of PV panels and wind turbines (Optimal case). The arrows

denote the MAC for bioenergy, nuclear, hydropower, concentrating solar power (CSP), and carbon capture and storage (CCS) in the literature³³. **b** Abatement of CO₂ emissions by building new PV and wind power plants by region over 2021–2040. **c, d** Effects of the spatiotemporal optimization in increasing the capacity of CO₂ emissions abatement (**c**) and reducing the costs of deploying PV, wind, CCS, and other types of low-carbon energy (a mix of bioenergy, geothermal, hydro, nuclear, and tidal wave) (**d**) in 2040. The areas of the pie denote the capacities of CO₂ emissions abatement by region in (**c**) and the costs of CO₂ emissions abatement by component in (**d**). Source data are provided as a Source Data file.

are constructed first to lower the costs of building more expensive power plants in the optimal path, which could reduce the costs of mitigation when decarbonizing global energy systems (see the effects of changing the order of construction on LCOE in Supplementary

Fig. 4). This strategy results in a gradual increase in investments leading up to the net-zero target in 2040 or 2070 (Supplementary Fig. 5). When achieving the net-zero target by 2070, the annual rates of installation during 2021–2040 are 0.32 TW y⁻¹ for PV power, 0.18 TW y⁻¹

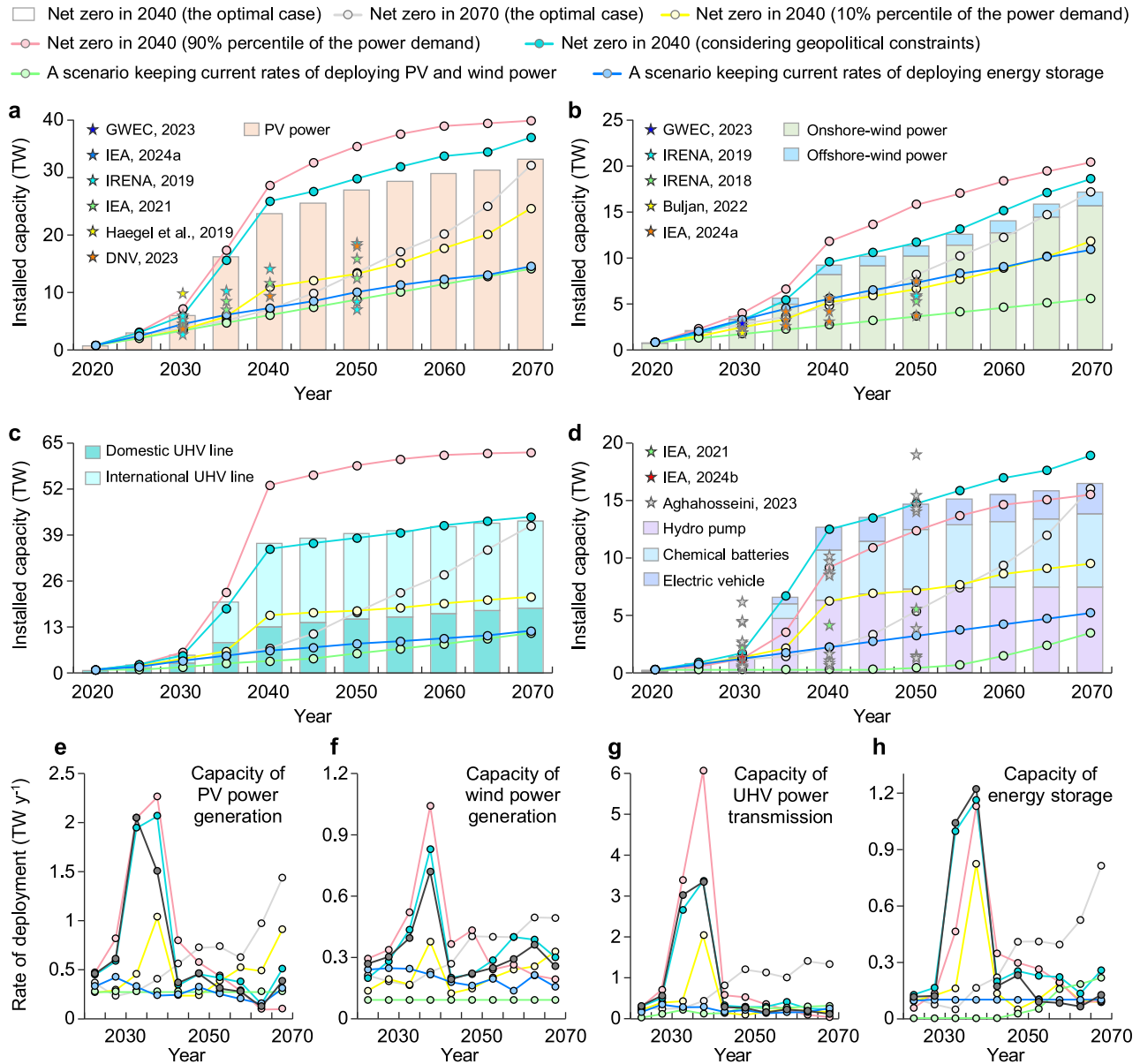


Fig. 4 | Comparison of the rates of deploying photovoltaic (PV) power, onshore and offshore-wind power, energy storage, and ultra-high-voltage (UHV) power transmission among various pathways of emissions. a–d Temporal changes in the global cumulative installed capacities of PV power (a), onshore and offshore wind power (b), domestic and international UHV lines (c), and energy storage by hydro pump, chemical batteries, and electric vehicles (d). The column denotes the prediction in our optimal case when achieving net-zero CO₂ emissions energy supply systems by 2040. We show the predictions when achieving the net-zero target by 2070, adopting a lower or higher projection of the power demand (i.e. using the 10% or 90% percentile in all future scenarios¹⁶), considering geopolitical constraints (i.e., considering the power transmissions only between countries in each continent and between Asian countries and Russia), keeping the current rate of deploying PV and wind power³⁶ during 2021–2023 or keeping the current rate of deploying energy storage^{38–40} during 2021–2023. We compare our estimate with

previous studies by the Global Wind Energy Council (GWEC) (2023)⁴³ based on a commitment by governments, industry, investors, and civil society at COP28, by the International Energy Agency (IEA) (2024a)⁴⁷ based on today’s policy settings and scenario of achieving net zero emissions by 2050, by International Renewable Energy Agency (IRENA) (2019)⁴² based on stated policies, announced pledges, and target of net zero emissions by 2050, by IEA (2021) based on the announced pledges⁴⁰, by Haegel et al.⁵⁰, by Det Norske Veritas (DNV) (2023)⁵¹, by IRENA (2018)⁴⁵, by Buljan (2022)⁴⁶, by IEA (2024b)⁴⁸ based on today’s policy settings and scenario of achieving net zero emissions by 2050, and by Aghahosseini et al.⁴⁹ based on an energy system model. **e–h** Comparison of the annual rates of deployment for PV (e), wind (f), power transmission by UHV lines (g), and energy storage (h) among different scenarios. Source data are provided as a Source Data file.

for onshore-wind power, 0.02 TW y⁻¹ for offshore-wind power, 0.1 TW y⁻¹ for energy storage, and 0.3 TW y⁻¹ for power transmission by UHV lines, which are close to the historical rates over 2021–2023 (i.e. 0.27 TW y⁻¹ for PV power³⁸, 0.09 TW y⁻¹ for onshore-wind power³⁸, 0.01 TW y⁻¹ for offshore-wind power³⁸, and 0.1 TW y⁻¹ for energy storage^{38–40}). In contrast, the rates of deployment need to be increased to meet the net-zero target by 2040, which should reach 1.15 TW y⁻¹ for PV power, 0.37

TW y⁻¹ for onshore-wind power, 0.05 TW y⁻¹ for offshore-wind power, 0.62 TW y⁻¹ for energy storage, and 1.8 TW y⁻¹ for power transmission by UHV lines.

The growth of PV and wind power needs to be further accelerated in the scenario with a larger demand for power to support economic growth, while geopolitical conditions could limit the range of power transmission between countries. In our optimal case, the capacity of

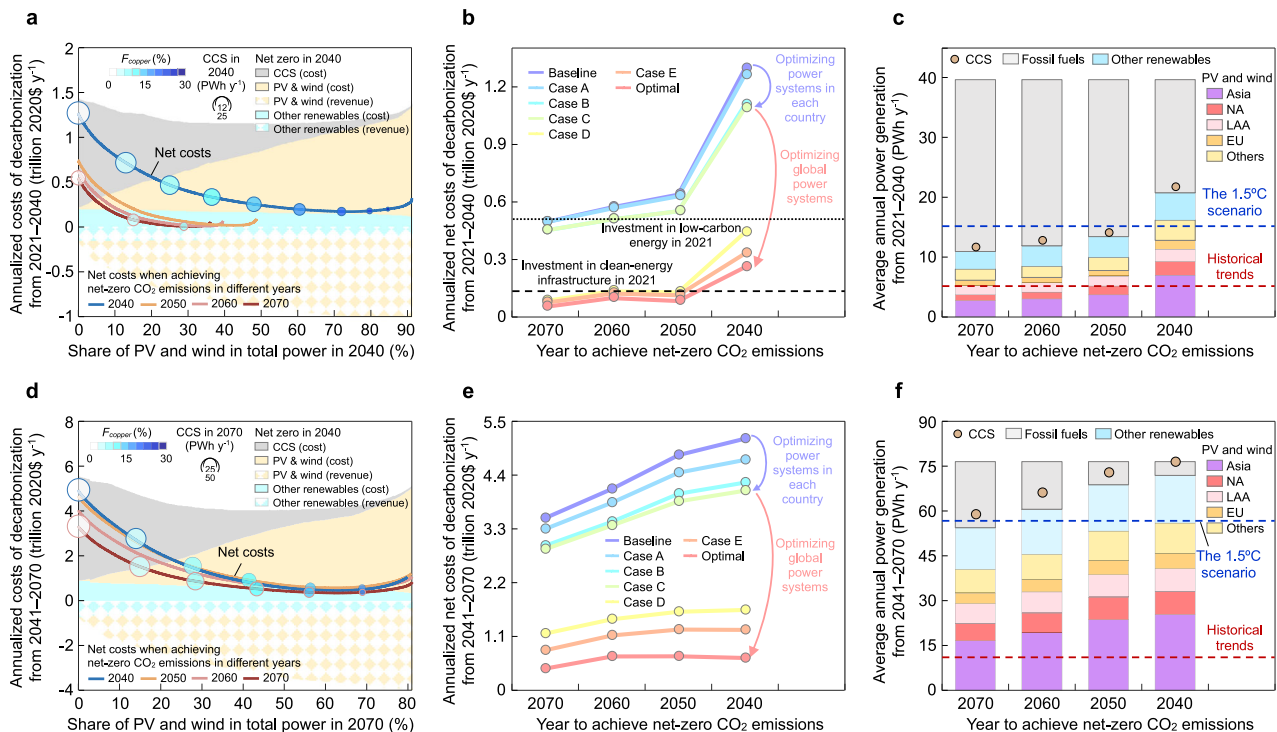


Fig. 5 | Costs of decarbonization of the power system to advance the time of achieving global net-zero CO₂ emissions by accelerating the penetration of photovoltaic (PV) and wind power. **a** Relationship between the share of PV and wind in total power supply achieved by 2040 and the annualized costs of decarbonization over the period of 2021–2040 when advancing the time of achieving net-zero CO₂ emissions from 2070 to 2040. The color of the circles denotes the fraction of copper production that is used to produce PV panels and wind turbines (F_{copper}), while the size of the circles denotes the capacity of carbon capture and storage (CCS) installed by 2040. **b, c** The estimated costs of decarbonization (**b**)

and total power generation (**c**) over the period of 2021–2040 when achieving net-zero CO₂ emissions in different years. **d–f** as (**a–c**), but for the period of 2041–2070. The dashed and dotted line in (**b**) indicates current low-carbon energy infrastructure⁵³ and low-carbon energy investment^{54,55} in 2021, respectively. In (**c, f**), the dotted blue line denotes the average PV and wind power capacities in all 1.5°C scenarios adopted by IPCC¹⁶, while the dotted red line denotes the predicted PV and wind power capacities in the scenario keeping the rate of deploying PV and wind power during 2011–2020 unchanged over the period of 2021–2070. Source data are provided as a Source Data file.

wind power installed by 2040 (9.2 TW) to meet the net-zero target by 2040 is higher than the estimates (2–7.6 TW) in previous studies^{43–47}. The capacity of energy storage needs to be increased from 2.1 to 12.7 TW to meet the net-zero target over 2021–2040, which is higher than the projection (10.3 TW) in previous studies^{40,48,49}. It indicates that these expensive technologies have to be deployed when meeting more ambitious climate targets¹⁶, which requires overcoming technological and economic barriers. In addition, our results highlight the importance of meeting the demand for materials, including copper, zinc, nickel, silicon, manganese, chromium, molybdenum, rare earths, cement, fiberglass, glass, steel, aluminum, lithium, cobalt, and graphite (Supplementary Table 2). There is a rapid growth in the consumption of materials when achieving the net-zero target by 2040, which is consistent with the projection a study published in 2022⁵². We predict that the demands for fiberglass, glass, and cobalt largely exceed the annual rate of production (Supplementary Fig. 6). The high demands for minerals and materials need to be met by enforcing an efficient utilization of materials with recycling to guarantee the energy security when integrating high shares of variable renewable energy into global power grids.

Costs of decarbonizing the energy supply systems

Costs of decarbonization to achieve net-zero CO₂ emissions influence the rates of decarbonizing power systems by phasing out fossil fuels², which determine the peak of global warming¹ and the probability of crossing climate tipping points^{3,4}. For comparison with previous models that did not account for the effects of spatiotemporal optimization^{19,21,22}, our currently developed model incorporates these

benefits by optimizing the dynamics of technological improvements, coordination of facilities for energy storage and power transmission, and development of regional supply chains for PV panels and wind turbines. When achieving net-zero CO₂ emissions energy supply systems in 2040, we predict the annualized net costs during 2021–2040 to decline from \$1.3 trillion y⁻¹ (i.e. 1.5% of global Gross Domestic Product (GDP) in 2020) in the baseline case to \$0.26 trillion y⁻¹ (i.e. 0.3% of global GDP in 2020) in our optimal case (Fig. 5). This is accompanied by a great expansion of PV and wind power from 2.4 PWh y⁻¹ in 2020 (i.e. 9% of the total power supply) to 38.7 PWh y⁻¹ in 2040 (i.e. 75.1% of the total power supply). The required investment in low-carbon energy can be substantially reduced by optimization, but the current low-carbon energy investment^{53–55} in 2021 cannot meet the requirement when meeting ambitious climate targets^{1,2}. We predict that annualized net costs during 2021–2040 decline from \$1.3, \$0.64, \$0.57, and \$0.49 trillion y⁻¹ in the baseline case to \$0.26, \$0.08, \$0.1 and \$0.05 trillion y⁻¹ in our optimal case when achieving net-zero CO₂ emissions in 2040, 2050, 2060 and 2070, respectively (Fig. 5b). We predict that achieving a higher rate of decarbonization will increase the costs of decarbonization moderately by adopting low-cost PV and wind power at sub-national scales in our optimal case due to the accelerated technological advances by learning³⁰. The share of PV and wind in global total power supply during 2021–2040 will increase from 15% in the baseline case to 40.8% in our optimal case (Fig. 5c), which requires upgrading global power systems and developing facilities of power transmission and energy storage. Considering the demand for minerals in the manufacture of PV panels and wind turbines, a rapid growth of PV and wind power will lead to a great expansion of the trade of

minerals across regions because the consumption of minerals such as copper and manganese in Asia and North America will heavily rely on the import from countries in South America and Africa (Supplementary Fig. 7). We predict that global capacities of energy storage will reach 6.2 TW for hydro pump, 4.3 TW for chemical batteries, and 2 TW for electric vehicles by 2040 (Supplementary Table 3). In addition, global capacities of power transmission will reach 12.4 TW within countries and 23.7 TW between neighboring countries by 2040 in our optimal case (Supplementary Table 4).

Demands for the lands, infrastructure, minerals and investments

We explore the requirements on land occupation, energy storage, power transmission, mineral consumption, and total investments by comparing two scenarios achieving net-zero CO₂ emissions by 2040 and 2070 in our optimal case (Table 1). When achieving net zero in 2040 rather than 2070, global capacities of PV and wind power plants built during 2021–2040 will increase from 10.3 to 31.5 TW, requiring additional lands of 12.5 mega hectare (Mha) for placing PV panels and 2.2 Mha for installing onshore wind turbines. The environmental impacts of installing PV panels and wind turbines are multifaceted, encompassing aspects including microclimate alterations, wildlife vulnerability, transformations of the type of land use, air pollution, habitat changes, and soil contaminations^{56,57}. In our optimal case, the total area of land installing PV panels and wind turbines is projected to reach 315,255 (~0.2% of global land area) square kilometer (km²) by 2070 when achieving the net-zero target by 2070. We identify 40%, 24%, 13%, and 8% of the area to be located in desert, grassland, open shrubland, and savanna lands, respectively (Supplementary Table 5). Although the direct area of land occupation by wind turbines is smaller than that by PV panels, the footprint of installing wind turbines could be remarkable when considering factors such as the visual impacts. When advancing the year achieving the net-zero target from 2070 to 2040, the fraction of biodiversity loss due to the installation of PV panels and wind turbines in 2040 increases from 0.08% to 0.18% in developing countries and from 0.09% to 0.2% for all countries (Supplementary Fig. 8).

The socioeconomic impacts of the energy transitions from fossil fuels to renewable energy deserve attention. Using our optimization model, we find that global employment in the power sector over 2021–2040 will increase from 142 million y⁻¹ to 276 million y⁻¹ when achieving the net-zero CO₂ emissions target by 2040 rather than 2070, where 2.6% of global total population (2.64% for developing countries and 2.26% for developed countries) will be working in the sectors related to power generation using renewable energy by 2040 (Supplementary Fig. 9). As a limitation, our model cannot consider how the availability of the skilled workforce and the problem of the increased unemployment in the fossil-fuel industries will influence the capacity of mitigation by deploying renewable energy. Energy transition will lead to a rapid growth in employment opportunities in low-carbon energy sectors, which requires increasing investment in human capital and diversification programs to support workforce training⁵⁸. Socio-economic barriers should be also overcome to change the structure of the workforce in the regions relying on fossil fuels as the main source of employment⁵⁹ and increase the geospatial mobility of the re-skilled fossil-fuel extraction workers⁶⁰. In addition, we find that power generation by PV and wind for developing and developed countries will reach 4.1 and 13.7 Megawatt-hour (MWh) y⁻¹ per capita in 2040 when achieving net-zero CO₂ emissions target by 2040, compared to 2 and 5.6 MWh y⁻¹ per capita in 2040 when achieving net-zero CO₂ emissions target by 2070, respectively (Supplementary Fig. 10). It indicates that achieving a more ambitious target of mitigation needs to overcome the economic and political barriers to improve the access to renewable energy. This could, in turn, improve the degree of energy equity by increasing access to modern energy in less developed countries.

Accelerating the growth of PV and wind power to advance the time of net zero from 2070 to 2040 increases consumption of materials and minerals during 2021–2040, including copper (by + 3.2 Mt y⁻¹ or 15.1% of global annual production), zinc (+ 1.3 Mt y⁻¹ or 9.7% of global annual production), nickel (+ 0.09 Mt y⁻¹ or 3.2% of global annual production), silicon (+ 3.3 Mt y⁻¹ or 37.9% of global annual production), manganese (+ 0.2 Mt y⁻¹ or 0.9% of global annual production), chromium (+ 0.1 Mt y⁻¹ or 0.3% of global annual production), and rare earth elements (+ 0.01 Mt y⁻¹ or 3.6% of global annual production) in the manufacture of PV panels and wind turbines (Supplementary Table 6). The annualized costs of decarbonization to achieve net zero in 2040 will be \$1.1 trillion y⁻¹ for PV and wind power and \$0.3 trillion y⁻¹ for CCS and other types of low-carbon energy during 2021–2040, which will be offset by revenue of \$1.1 trillion y⁻¹ by replacing fossil fuels. Notably, the present value of additional costs when achieving net zero in 2040 rather than 2070 amounts to \$6 trillion in the optimal case, which is about 25.2% of the benefits (i.e. \$20 trillion in 2010 US dollars or \$23.7 trillion in 2020 US dollars) from mitigating global warming from 2 to 1.5 °C that is predicted in an integrated assessment study³. In our optimal case, investments in low-carbon energy (PV, wind, CCS, and other types of low-carbon energy) need to increase from \$1.01 trillion over 2021–2025 to \$8.33 trillion over 2036–2040 to achieve an energy supply system with net-zero CO₂ emissions by 2040. The investments in renewable energy have increased from \$0.39 trillion y⁻¹ in 2020 to \$0.61 trillion y⁻¹ in 2023 in Bloomberg's report⁵⁵, which are consistent with an increase from \$0.35 trillion y⁻¹ in 2020 to \$0.50 trillion y⁻¹ in 2022 in another assessment⁵⁴. We provide a summary of climate policies and environmental regulations aimed at facilitating the deployment of renewable energy projects in various countries (Supplementary Table 7). Notably, the diverse policy and regulatory frameworks, augmented taxation on fossil fuels, incentives driven by fiscal policies, global networks of technological diffusion, and the financial backing by carbon markets and international funds can expedite the transitions from fossil fuels to renewable energy dominated by PV and wind power.

Trade of minerals and transmission of power across regions

A study published in 2022 noticed a significant effect of establishing a globalized supply chain of PV panels in reducing 25% of total costs by 2030²⁷. We examine the effects of accelerating the global deployment of PV and wind power and increasing the capacities of power transmission and energy storage (i.e. the difference between the baseline case and Case C), while we further examine the effects of increasing the trade of minerals and power transmission between countries, and developing regional supply chains for PV panels and wind turbines (i.e. the difference between Case C and the optimal case) (Fig. 3). Beyond our optimal case, we consider an idealized case of “Opt_GSC” by extending the supply chains of PV panels and wind turbines from regional scales to global scales (see the underlying assumptions in Supplementary Table 1). In this case, the international flow of minerals and transmission of electricity between countries can further reduce the cost of decarbonization of the power sector by overcoming geographic constraints and technical challenges^{61,62} (Fig. 6). Notably, maximizing the number of relationships between countries leads to additional export of manganese by 132 kiloton (kt) y⁻¹ and an increase in the transmission of electricity by 4.1 PWh y⁻¹, where a flow of finance by \$85.9 billion y⁻¹ will be embodied in the supply chains of PV panels and wind turbines over the period of 2021–2040 (Fig. 6a–c). We identify the largest export of manganese from Africa to Europe by 17 kt y⁻¹ (see the flow of manganese, copper, and silicon between countries in Supplementary Fig. 7). The annualized net costs saved by increasing the international flow of materials, minerals, and transmission of electricity amount to \$0.19 trillion y⁻¹ in Asia, \$0.11 trillion y⁻¹ in Europe, \$0.04 trillion y⁻¹ in North America, \$0.09 trillion y⁻¹ in Africa and Latin America, or \$0.55 trillion y⁻¹ as global total during 2021–2040

Table 1 | Requirements on the installed capacities of photovoltaic (PV) and wind power, power transmission, energy storage, land occupation, mineral supply, and investments when advancing the time to achieve energy supply systems with net-zero CO₂ emissions from 2070 to 2040

Year to achieve net-zero CO ₂ emissions	Period of the energy transition	Installed PV capacity (TW)	Installed wind power capacity (TW)	Capacity of power transmission (TW)	Capacity of energy storage (TW)	Lands required for installing PV panels (Mha)	Lands required for installing onshore-wind turbines (Mha)	Total demand for mineral (taking copper as an example) (Mt y ⁻¹)	Consumption of copper as a percentage to annual production (%)	Annual costs of PV and power (trillion 2020\$ y ⁻¹)	Annual costs of carbon capture and storage (CCS) and other types of low-carbon energy (trillion 2020\$ y ⁻¹)	Annual revenue of replacing fossil fuels (trillion 2020\$ y ⁻¹)	Present value of costs of deploying PV, wind, CCS, and other types of low-carbon energy (trillion 2020\$)	Present value of revenue of replacing fossil fuels (trillion 2020\$)	Present value of net costs under a discount rate of 3% in the baseline case (trillion 2020\$)
2040	2021–2025	2.27	1.36	1.55	0.58	1.67	0.67	2.22	10.57	0.18	0.05	-0.23	1.01	-0.98	0.04
	2026–2030	3.02	1.53	2.81	0.60	2.27	0.76	2.76	13.17	0.56	0.18	-0.68	2.90	-2.66	0.24
	2031–2035	10.23	1.99	15.06	5.20	7.67	0.97	7.22	34.41	1.25	0.36	-1.32	5.43	-4.48	0.95
	2036–2040	7.51	3.61	16.65	6.11	5.57	1.79	6.73	32.09	2.26	0.57	-2.17	8.33	-6.38	1.95
	2021–2040	23.03	8.49	36.08	12.49	17.18	4.19	4.73	22.56	1.06	0.29	-1.10	17.66	-14.50	3.17
	2041–2070	9.47	7.96	6.34	3.81	6.96	4.00	1.74	8.31	3.31	1.12	-3.77	47.54	-39.80	7.73
	2021–2070	32.50	16.45	42.41	16.29	24.13	8.19	2.94	14.01	2.41	0.79	-2.70	65.20	-54.30	10.90
2070	2021–2025	1.80	1.07	1.40	0.52	1.31	0.53	1.74	8.30	0.15	0.03	-0.17	0.76	-0.73	0.03
	2026–2030	1.13	0.93	1.21	0.37	0.83	0.47	1.26	6.02	0.38	0.10	-0.45	1.89	-1.78	0.11
	2031–2035	1.38	0.84	1.29	0.24	1.04	0.42	1.30	6.22	0.57	0.18	-0.70	2.57	-2.38	0.19
	2036–2040	1.99	1.16	2.17	0.82	1.49	0.57	1.96	9.33	0.80	0.29	-0.98	3.19	-2.88	0.31
	2021–2040	6.30	4.00	6.07	1.96	4.66	1.99	1.57	7.46	0.47	0.15	-0.57	8.41	-7.77	0.64
	2041–2070	25.12	12.39	34.45	13.83	18.70	6.18	3.74	17.81	2.33	0.80	-2.68	31.01	-26.73	4.28
	2021–2070	31.43	16.39	40.51	15.78	23.36	8.17	2.87	13.67	1.59	0.54	-1.84	39.42	-34.50	4.92

The results are derived from our optimal case except for the present value of net costs (the last column shows the estimate in the baseline case).

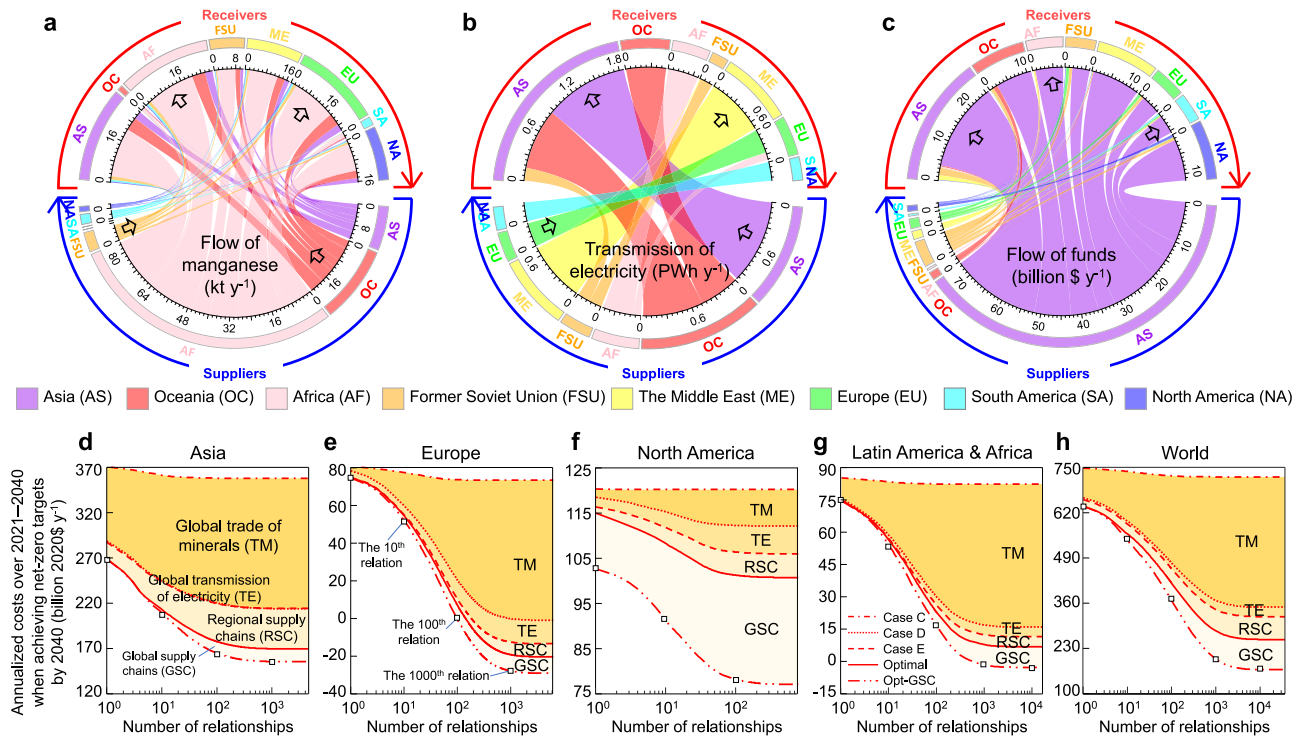


Fig. 6 | Effects of optimizing global power systems in reducing the costs of decarbonization when achieving net-zero CO₂ emissions by 2040. **a–c** Global flow of manganese as an example for minerals (**a**), global transmission of power (**b**), and global flow of funds embodied in the supply chains of PV panels and wind turbines (**c**) over the period of 2021–2040 in the “Opt_GSC” case (see assumptions for this scenario in the text). **d–h** Total costs of decarbonization to achieve energy

supply systems with net-zero CO₂ emissions by 2040 in Asia (**d**), Europe (**e**), North America (**f**), Latin America and Africa (**g**), and the World (**h**) when increasing the number of relationships between countries to optimize global trade of minerals, transmission of power, and supply chains of PV panels and wind turbines. Source data are provided as a Source Data file.

(Fig. 6d–h). We estimate the net costs by subtracting the revenue of replacing fossil fuels from the costs of deploying PV and wind power, where the former depends on the prices of fossil fuels. We observe that the current prices of fossil fuels in European countries are higher, averaging \$0.06 kWh⁻¹, compared to those in other regions (e.g., \$0.04 kWh⁻¹ in Asia) (Supplementary Data 1). When achieving energy supply systems with net-zero CO₂ emissions by 2040, the annualized revenue from replacing fossil fuels during 2021–2040 will reach \$365 billion y⁻¹ if we adopt the prices of fossil fuels in Europe, which decreases to \$280 billion y⁻¹ if the global average prices of fossil fuels are adopted. In this case, annual costs are projected to be \$346 billion y⁻¹ (\$106 billion y⁻¹ for PV and wind power and \$240 billion y⁻¹ for CCS and other types of low-carbon energy) along the optimal path. Consequently, the net costs are negative (-\$20 billion y⁻¹) in Europe when using the prices of fossil fuels in Europe, which will increase to \$65 billion y⁻¹ when applying the global average price of fossil fuels in the optimal path. We predict that the production of minerals cannot meet the demand when achieving the net-zero target by 2040 for most European countries (e.g. the demand for 22.5 Mt copper per year v.s. the production of 11 Mt copper per year in 2040 for Germany, and the demand for 46.7 Mt copper v.s. the production of 22 Mt copper per year in 2040 for France). As a result, the net costs of decarbonization of the power sector in Europe can be reduced from \$73 billion y⁻¹ in Case C to -\$1 billion y⁻¹ in Case D by increasing the import of minerals, and further to -\$29 billion y⁻¹ in “Opt_GSC” case by importing electricity, PV panels and wind turbines produced in other regions (Fig. 6e).

Discussion

Achieving net-zero CO₂ emissions by 2040 remains challenging due to the slow progress in phasing out fossil fuels under current policies or conditional NDCs^{1–6,10,11,14}. We explore a strategy of accelerating the

penetration of PV and wind power through spatiotemporal optimization by combining geospatial data²³ with dynamics of cost reductions under technological improvements²⁰. Our optimization effectively narrows the gap between the supply of PV and wind power¹⁹ and the demand for electricity when phasing out fossil fuels to meet the 1.5 °C target¹⁶ by minimizing the levelized cost of electricity. Our identification of low-cost PV and wind power generation at sub-national scales leads to a moderate increase in the costs of decarbonization to advance the time of meeting net-zero targets from 2070 to 2040. Compared to previous models without spatiotemporal optimization^{19,21,22}, our study provides an empirically grounded estimate of the costs of decarbonization of the power sector to estimate the maximal capacities of PV and wind power and the associated costs.

Accelerating the integration of solar and wind power in global power systems is important for meeting ambitious climate targets⁴⁰. Recent studies have made progress in identifying scenarios with high capacities of PV and wind-power generation at regional scales^{23,37}, examining the feasibility of integrating a high proportion of solar and wind energy in the power grids^{34,36}, quantifying the effects of constructing the infrastructure for power transmission and energy storage³⁸, evaluating the demand for minerals in the deployment of renewable energy⁶³, and estimating the financial gap of deploying renewable energy³⁵. From a global aspects, our study explores the pathway of strongly accelerating the deployment of PV and wind power by considering geographic limitations by solar radiation and wind speed, efficiency of energy conversion, suitability of lands for power generation, geological constraints of energy storage, demand for materials, costs of power transmission and energy storage, effects of technological advances on module costs, and supply chains of PV panels and wind turbines. Our results suggest that the increased costs of decarbonization to accelerate the growth of PV and wind power

could be lower than the estimated climatic damage in the literature³. Our optimization exercises provide insight into some global challenges when accelerating climate mitigation. First, deeper decarbonization of power systems increases the marginal abatement costs due to the rising physical and technological constraints, such as higher land requirements, mineral consumption, and lower efficiencies of PV and wind power generation given the limitation of power transmission and energy storage. Second, high maintenance costs may arise when PV and wind power grow at unprecedented rates in our optimal case, such as the need to place PV panels over the vast desert areas in China²³ or ensuring the safety of wind turbine installation and grid connection in Europe and North America⁶⁴. Lastly, we highlight the importance of ensuring the global flow of electricity, trade of minerals, and international funds, whereas the potential impacts of geopolitical conflicts on the supply chains of materials and minerals^{27,62} deserve attention.

Some caveats in our model deserve attention. First, we assume that international cooperation can facilitate the transmission of power and the trade of minerals between countries, but the feasibility of these aspects might be hindered by geopolitical reasons in the future. Changes in geopolitical conditions due to regional conflicts such as the Ukraine War remain uncertain, which could affect the projection of total power demand, availabilities of renewables other than PV and wind, inter-regional power transmissions, and international trades of minerals. Second, we optimize the spatiotemporal distributions of PV and wind-power plants, energy storage, and power transmission based on the hourly variations of solar radiation, wind speed, temperature, and the profiles for power demand using forecast data from Integrated Assessment Models (IAMs) assessed by IPCC⁵. These meteorological and socioeconomic conditions, however, could change dramatically due to climate change as well as the actions taken globally to tackle the problem of climate change, which are not explicitly considered in our model. While we strive to minimize the costs of unit-effective power generation by optimizing the strategies of power-plant construction, energy storage, and power transmission based on the spatiotemporal variations in power generation and the demand for power, it is important to note that the outcomes of our optimization are subject to deviation when considering variabilities in future climate change and shifts in the demand for power. Last but not least, there are factors which could affect the deployment of power generated by low-carbon energy but have not been considered in our current model, such as the availability of skilled workforce, re-distribution of labors in space, geopolitical constraints, available investments in low-carbon energy, inefficient utilization of materials, physical constraints to further cost reduction by technological advances, interactions between climate change and PV and wind energy, and ecological impacts of constructing PV and wind-power plants. Acknowledging these drawbacks and the associated uncertainties underscores the need for ongoing refinement and adaptability within the optimization framework to effectively address evolving environmental and energy consumption dynamics, ensuring the continued relevance and efficacy of the proposed strategies in a changing energy landscape.

Energy security and geopolitical crisis may pose additional obstacles to threaten the safety of energy infrastructure because climate change might increase the frequency of regional conflicts in the second half of this century once mitigation is delayed⁶⁵. We find that expanding the supply chain from regional to global levels could remove one-third of the costs of mitigation, but it would largely increase the flow of minerals and materials (e.g., almost half of the manganese will be exported from Africa to other regions in the world) (Fig. 6). This would require efforts to overcome barriers in the diffusion of low-carbon technologies due to trade-distortive subsidies, local protectionism and geopolitical issues^{62,66}. We predict that the development of global supply chains might increase the monopoly of renewable energy in countries with price advantages on world markets (e.g., three-fourths of the fund flow embodied in the trade of PV panels

and wind turbines will be originated from few countries in East Asia). This could accelerate the rate of technological advances to reduce the costs of renewable energy but has a risk to reduce energy security in countries relying on the import of technologies²⁷. As a limitation in our model, we cannot resolve the structure of capital and workforce at a country level, so it is unclear whether the manufacture of PV panels and wind turbines can reach the projected levels by securing the demands for capital and labor (e.g., the availability of skilled workforce^{58,60}). Nevertheless, our model with a high flexibility of considering the impact of individual factors provides a useful tool to explore the effect of increasing the coverage of supply chains in reducing the costs of mitigation to meet the global climate targets (e.g., see the difference among Case E without regional supply chains, the optimal case with regional supply chains, and the Opt_GSC case with global supply chains). Our modeling results suggest that it is not too late to achieve global energy systems with net-zero CO₂ emissions by 2070 or even by 2040, but long-term planning in deep decarbonization requires a structural reform to finance a stable transition toward low-carbon energy with global joint efforts.

Methods

Geospatial data used in this study

To estimate the maximal capacity of photovoltaic (PV) and wind-power generation^{67–69}, we collect global geospatial data including clear-sky solar irradiance, friction velocity, zero-plane displacement height, length of roughness, surface air temperature, administrative boundaries, types of land cover, slope of ground, altitude, latitude and longitude of pixels, water depth, shipping routes, mineral production, terrestrial and marine natural reserves, specification of PV panels and wind turbines, terrestrial carbon sink, and soil carbon content (see the sources of data in Supplementary Table 8). We filter the pixels that are suitable for installing PV panels or placing wind turbines based on the type of land cover, ground slope, maximal monthly solar radiation, maximal monthly average capacity factor, maximal monthly temperature, altitude above sea level, depth of water, distribution of terrestrial and marine reserves, territorial sea area, and shipping routes (see the thresholds of filtering data in Supplementary Table 9). To estimate the capacity of power generation by PV panels in each pixel, we compile the gridded data of hourly solar radiation and ground-level air temperature at a spatial resolution of 0.5° in latitude and 0.625° in longitude in the period of 2012–2020 from the NASA's Goddard Earth Observing System Model, version 5 Forward Processing database⁷⁰, which are re-projected on the map at a spatial resolution of 0.0083° in latitude and 0.033° in longitude by assuming homogeneity in the 0.5° × 0.625° pixels. Similarly, we compile the gridded data of hourly friction velocity of wind speed at a spatial resolution of 0.5° in latitude and 0.625° in longitude over the period of 2012–2020 from the Modern-Era Retrospective analysis for Research and Applications, Version 2 (MERRA-2) data set⁷⁰, which are re-projected on the map at a spatial resolution of 0.0083° in latitude and 0.033° in longitude by assuming homogeneity in the 0.5° × 0.625° pixels.

To constrain the maximal number of pixels that are used for installing PV panels or wind turbines, we compile the boundaries of countries in 192 countries from the global administration data set⁷¹, which are re-projected on the map at a spatial resolution of 0.0083° in latitude and 0.033° in longitude. We compile the gridded data of land cover from the Moderate Resolution Imaging Spectroradiometer Land Cover Type 1 data set³¹, which categorizes all land pixels into forests, shrubland, savanna, grasslands, wetlands, croplands, urban and built-up lands, natural vegetation mosaics, snow and ice, desert, and water bodies. We compile the data for locations of terrestrial ecological reserve at a spatial resolution of 0.001° in latitude and 0.001° in longitude from the Resource and Environment Science and Data Center⁷² and the slope of ground at a spatial resolution of 0.001° in latitude and 0.001° in longitude from the Shuttle Radar Topography

Mission data set⁷³. We compile the zero-plane displacement height and the surface roughness at a spatial resolution of 0.5° in latitude and 0.625° in longitude from NASA's Goddard Earth Observing System Model, version 5 Forward Processing data set⁷⁰. To determine the location of offshore wind power plants, we compile the data of territorial sea area from the Maritime Boundaries Geodatabase⁷⁴, depth of water from the Radar Topography Mission Global Enhanced Slope Database⁷³, and geo-locations of the marine ecological reserve from the National Marine Data and Information Service^{72,75}. In addition, we compile the global gridded data of sulfur dioxide (SO_2) emission from shipping during 2012–2020 from the Modern-Era Retrospective analysis for Research and Applications (version 2) database⁷⁰ to identify the routes of shipping³⁶.

To predict the power demand during 2021–2070, we compile the projected data of total power demand for 2021–2070 by country for Pakistan, South Korea, South Africa, Colombia, Argentina, Brazil, Canada, China, India, Indonesia, Japan, Mexico, Russia, and the USA¹³. For the remaining countries, we compile the data of total power demand for 2021–2070 in eleven regions including North America, Eastern and Western Europe, Pacific Organization for Economic Cooperation and Development (Pacific OECD), Reforming Economies of Eastern Europe and the Former Soviet Union, Centrally-planned Asia, South Asia, Other countries of Asia, Sub-Saharan Africa, the Middle East, Latin America and the Caribbean, and the rest of the World from the median of forecast simulation in all future scenarios from AR6 Scenarios Database hosted by International Institute for Applied Systems Analysis (IIASA) (ref.¹⁶). By using the national power consumption in 2020⁷⁶ as a proxy in each region, the total power demands in these regions are disaggregated into 178 countries whose power demands aren't predicted by IIASA. We disaggregate the national power demand during 2021–2070 in 192 countries to 3,639 provinces or states using the gridded GDP in 2015 as a proxy in each country. Global gridded data of GDP are compiled at a spatial resolution of $0.0083^\circ \times 0.0083^\circ$ from the Human Development Index database⁷⁷. To predict the hourly power demand in each province or state, we compile the hourly power load profiles in 34 provinces in China in 2018 from the National Development and Reform Commission database⁷⁸, the hourly power load profiles in 50 states in the USA in 2020 from the U.S. Energy Information Administration¹⁷, and the hourly power load profiles in the remaining 190 countries in 2015 from the Country-Level Detailed Global Electricity (PLEXOS-World) database⁷⁹.

In addition to geospatial data used in the calculation of PV and wind power generation, we compile data to predict the power generation from other sources of low-carbon energy (bioenergy, geothermal, hydro, nuclear, and tidal wave). We compile the average capacities of renewable energy other than PV and wind power from the forecast simulations of five independent integrated assessment models (AIM, GCAM, MESSAGEix, REMIND, and WITCH) that had been adopted by IPCC (Intergovernmental Panel on Climate Change) in the 2°C scenarios¹⁶. To constrain the capacities of PV and wind power by the supply of minerals, we compile the national data of reserve and annual production of copper, zinc, nickel, silicon, manganese, chromium, and rare earth elements in 2020 from the U.S. Geological Survey Global Database⁸⁰. To account for the difference in technological improvements between countries²⁷, we compile the learning rates for PV, wind, CCS, and other sources of low-carbon energy from measurements in 26 countries during the period of 1981–2020 (Supplementary Table 10). Lastly, we compile capital costs of PV panels and wind turbines reported in 50 countries and 8 regions (Supplementary Table 11), the prices of coal, oil, and gas in 34 countries (Supplementary Data 1), the calorific values of coal, oil, and gas in 16 countries (Supplementary Data 2), the CO_2 emission factors of coal, oil and gas in 30 countries (Supplementary Data 3), and the national discounting rates in 192 countries (Supplementary Data 4), which are used in our spatially explicit model. For countries with a lack of data, we apply the

regional averages based on data above from countries with data in each region.

Spatiotemporal optimization of future photovoltaic and wind-power plants

We follow five steps to optimize the spatiotemporal distributions of future PV and wind-power plants. An overview of our optimizing procedures is illustrated in Fig. 1. The methods and assumptions of our optimization are summarized below, while the detailed formulations are provided in the following sections.

First, we seek the best strategy of installing PV panels or wind turbines to achieve the maximal capacity of power generation in each county²³. In each county, we maximize the capacity of power generation among five strategies: building one power plant (i), building two plants by equally dividing the county into the south and north (ii), or the east and west (iii), and building four plants by equally dividing the county into the east, south, west, and north (iv), or the southeast, southwest, northwest, and northeast (v). We obtain the locations of 22,821 potential PV and wind-power plants, which are distributed in 192 countries.

Second, we divide the area used to construct a new power plant into pixels at a resolution of 0.0083° in latitude and 0.0333° in longitude. On one hand, increasing the number of pixels to build a larger power plant increases the efficiency of infrastructure utilization (e.g. installation work, permitting and commission, planning, and transformers) and thus reduces the LCOE of the power plant. On the other hand, increasing the number of pixels reduces the effective power generation ratio when using pixels with lower potentials of PV and wind-power generation, which increases the LCOE of the power plant. We develop algorithms to estimate the dependence of LCOE of each power plant on the number of pixels installing PV panels and wind turbines by accounting for the density of installing PV panels or wind turbines, and we optimize the number of pixels installing PV panels and wind turbines²¹. This algorithm allows us to optimize the number of pixels installing PV panels and wind turbines to minimize the LCOE of each newly built power plant (see Eq. (1)).

Third, we optimize the capacity of energy storage at an interval of one hour to minimize the LCOE when achieving a target of total CO_2 emissions reduction. Based on the hourly fluctuations in PV and wind power generation, as well as the demand for power, any surplus electricity at a given time step will be stored for future use. This stored electricity will be utilized at the appropriate time steps when electricity production falls short of meeting the demand. We assume that chemical batteries are implemented for charging electrical vehicles. In the other sectors, we consider two strategies of energy storage for each PV or wind-power plant: hydro pump and chemical batteries (see Supplementary Method 6 for a detailed comparison of the lifetime and costs of energy storage between hydro pump and chemical batteries). We assume that chemical batteries can be charged and discharged for 6000 times over a lifetime of 15 years⁸¹ and that pumped-hydro storage can be charged and discharged for 1 time per day over a lifetime of 50 years⁸². We assume that the installation of a hydro pump would be limited by the maximal capacity of the exploitable closed-loop, off-river pumped hydro in each country⁸³. Taking into consideration the topographical features, Stocks et al.⁸³ developed the algorithms to identify 616,000 economically viable closed-loop, off-river sites suitable for pumped hydro installations by employing high-resolution digital elevation models and found a global total storage capacity of 23,000 TWh. These sites are classified into five classes, where class A, representing the most economically feasible option are considered to be the potential sites of hydro pump in our model. Considering the dependence of LCOE on the capacity of energy storage, we seek the optimal strategy of energy storage to minimize the LCOE of each power plant when meeting a national target of total CO_2 emissions reduction.

Fourth, we consider the effects of increasing the capacity of power transmission in each country using three strategies of ultra-high-voltage (UHV) power transmission for each PV or wind-power plants: ± 800 kV direct current (DC), ± 1100 kV DC, and 1000 kV alternating current (AC) (see Supplementary Method 5 for a detailed comparison of the costs of construction and power transmissions among the three strategies). We consider the current capacity of power transmissions between countries (e.g., between countries in Europe and between the USA and Canada in North America) in the baseline scenario. We further consider the transmission of power between neighboring countries in the same continent and some neighboring continents (including between Europe and the Former Soviet Union, Asia and the Former Soviet Union, the Middle East and the Former Soviet Union, North Africa and Europe, the Middle East and South Asia, the Middle East and Europe, Pacific Developed region and Southeast Asia, and the Middle East and North Africa)^{83–85} in our optimal case. We estimate the hourly transmission of electricity by assuming that power generation by PV and wind-power plants in a region is used to meet the regional power demand before being transmitted to other regions. We consider the hourly power generation and demand based on the Coordinated Universal Time in each province or country, allowing us to account for differences in the daytime and nighttime between various time zones. When the demand for power in a region has been satisfied, the surplus power will be transmitted to another region by building four substations in the centers of the northwest, southwest, northeast, and southeast of the country. If there is an UHV line for power transmission between countries, the surplus power will be transmitted to the closest country in the same or neighboring continent. Considering the dependence of LCOE on the capacity of power transmission, we seek the optimal strategy of power transmission to minimize the global LCOE of PV and wind-power generation when meeting a target of global CO₂ emissions reduction.

Lastly, we optimize the year to build each PV or wind-power plant by solving an LCOE-minimization problem (shown as Eqs. (1) to (6)) of all power plants when achieving net-zero CO₂ emissions energy supply systems. We apply Wright’s law by assuming that the effects of technological advances can reduce the costs of producing PV panels, wind turbines, mounting material, secondary equipment, inverters, grid connection, installation work, permitting and commission, planning, transformer, and cable by accumulating the capacity of power generation²⁰. Considering the dependence of LCOE on the capacities of PV and wind-power plants built by region at an interval of 5 years, we optimize the capacities of PV and wind-power plants over time to minimize the LCOE of all PV and wind-power plants.

Minimization of the levelized cost of electricity

We estimate the levelized cost of electricity (LCOE) as the normalized present value of the total costs that is divided by the power generation over the lifetime of power plants²³ to account for the competition of PV and wind power with CCS and other sources of low-carbon energy (bioenergy, geothermal, hydro, nuclear and tidal wave). We optimize the capacity of each built PV or wind power plant, the strategy of energy storage, the type of electricity transmission, and the construction period for PV and wind power plants to minimize the LCOE (M_ϑ) by solving a cost-minimization problem in each country, which is constrained by the supply of minerals and the demand for electricity:

$$\min_{\vartheta, n_x, t_x, s_x, \kappa_x, R_y, E_z} M_\vartheta = \frac{(V_\vartheta + A_\vartheta) \cdot \left[1 + R_y \cdot \sum_{t_f=1}^{T_f} \frac{1}{(1+r_d)^{t_f}} \right] + G_\vartheta \cdot \sum_{t_g=1}^{T_g} \frac{1}{(1+r_d)^{t_g}} + \sum_{z=1}^7 E_z \cdot m_z \cdot \sum_{t_f=1}^{T_f} \frac{1}{(1+r_d)^{t_f}}}{E_\vartheta \cdot \sum_{t_f=1}^{T_f} \frac{1}{(1+r_d)^{t_f}}} \quad (1)$$

$$V_\vartheta = \sum_{q=1}^{N_q} \sum_{x=1}^{n_q} V_x(n_x, \sigma_x, \varphi_x), x \in q \quad (2)$$

$$E_\vartheta = \sum_{h=1}^{8760} \left[\sum_{q=1}^{N_q} \sum_{x=1}^{n_q} E_{x,h}(n_x) - \eta_{tra} \Theta_h - \eta_{store} \Lambda_h \right] + \sum_{z=1}^7 E_z, x \in q \quad (3)$$

$$\Theta_h = \sum_{q=1}^{N_q} \max \left[0, \sum_{x=1}^{n_q} E_{x,h}(n_x) - M_{q,h} \right] = \sum_{q=1}^{N_q} U_{q,h}, x \in q \quad (4)$$

$$\Lambda_h = \sum_{q=1}^{N_q} \max \left[0, \sum_{x=1}^{n_q} E_{x,h}(n_x) + U_{q,h} - M_{q,h} \right], x \in q \quad (5)$$

$$\Psi_\zeta = \sum_{q=1}^{N_q} \sum_{x=1}^{n_q} E_{x,h}(n_x) \cdot \chi_\zeta < \Omega_\zeta, x \in q, \zeta = 1, 2, \dots, 7 \quad (6)$$

where ϑ is a new PV or wind plant ($\vartheta = 1$ to 22,821), x is a PV or wind plant built before the plant ϑ , z is a type of low-carbon other than PV or wind energy (i.e. $z=1-6$ for bioenergy, geothermal, hydro, nuclear, tidal wave, and CCS, respectively), n_x is the number of pixels installing PV panels or wind turbines in a plant x , t_x is the time of building a plant x , s_x is the option of energy storage (1 for hydro pump and 2 for chemical batteries) when building a plant x , κ_x is the option of power transmission (1 for ± 800 kV DC, 2 for ± 1100 kV DC, and 3 for 1000 kV AC), E_z is the power generation by low-carbon energy z , V_ϑ is the initial investment in PV and wind plants when building a plant ϑ , R_y is the ratio of O&M costs to initial investment, A_ϑ is the costs of power transmission using UHV lines when building a plant ϑ (The geographic information for 1,214 UHV lines included in our study are listed in Supplementary Data 5), G_ϑ is the costs of energy storage by hydro pump or chemical batteries when building a plant ϑ , r_d is the discounting rate, T_f is the average lifetime of PV or wind-power plants, L_g is the average lifetime of energy storage, t_f is a year in the operation of a plant x , t_g is a year in the operation of energy storage, m_z is the LCOE for a low-carbon energy other than PV or wind power, E_ϑ is total power generation by low-carbon energy when building a plant ϑ , q is a region in a country, N_q is the number of regions in a country, n_q is the number of PV or wind power plants in a region q , σ_x is the fraction of cost reduction due to technological improvements, φ_x is the fraction of cost reduction by developing regional or global supply chains, V_x is the initial investment required to build a plant x , h is a hour, $E_{x,h}$ is the hourly power generation in a plant x , Θ_h is the hourly transmission of electricity, Λ_h is the hourly energy storage, η_{tra} is the fraction of electricity loss in the power transmission, η_{store} is the fraction of electricity loss in the processes of energy storage, $M_{q,h}$ is the hourly consumption of electricity in a region q , $U_{q,h}$ is the hourly transmission of electricity from other regions to the region q , ζ is a mineral (i.e. $\zeta=1-7$ for copper, zinc, nickel, silicon, manganese, chromium, and rare earth elements, respectively), χ_ζ is the unit consumption of a mineral ζ in the production of PV panels or wind turbines, Ψ_ζ is the total consumption of a mineral ζ , and Ω_ζ is the supply of a mineral ζ . All the variable descriptions are listed in Supplementary Table 12.

We estimate the supply of minerals as the sum of production and import minus export by country. The average ratio of annual O&M costs to initial investments (R_y) is 1% for PV plants⁸⁶ and 3% for onshore and offshore wind plants⁸⁷. We adopt a lifetime of 25 years for PV and wind plants⁸⁸, 50 years for energy storage when using hydro pump²³, and 15 years for energy storage when using chemical batteries⁸² (Supplementary Table 13). By solving the cost-minimization problem, a PV or wind plant, a type of low-carbon energy (bioenergy, geothermal, hydro, nuclear, tidal wave) or CCS with the lowest marginal abatement cost (MAC, defined as the cost of reducing one more unit of CO₂

emissions) will be deployed to reduce CO₂ emissions by replacing fossil fuels. By adopting the average estimate in the literature^{33,89,90}, we consider that MAC are \$130.85 per tCO₂ for CCS, \$47.09 per tCO₂ for biomass, \$7.30 per tCO₂ for geothermal, \$2.25 per tCO₂ for hydro-power, \$17.01 per tCO₂ for nuclear energy, and \$200.00 per tCO₂ for tidal wave in 2020, which will decline over time due to technological improvements. Detailed methods used to estimate the hourly power generation ($E_{x,h}$) in a PV, onshore, and off-shore wind-power plant are described in the Supplementary Methods 1–3. Detailed methods used to estimate the investment costs of building the PV and wind power plants (V_{δ}), costs of electricity transmission using UHV lines (A_{δ}), and costs of energy storage using hydro pump or chemical batteries (G_{δ}) are described in the Supplementary Methods 4–6. Detailed methods used to estimate the fraction of cost reduction due to technological improvements (σ_x) and supply chains (φ_x) are described in the following text.

Cost reduction due to technological advances

We consider the effects of technological advances in reducing the costs of PV panels, wind turbines, mounting material, secondary equipment, inverter, grid connection, installation work, permitting and commission, planning, transformer, and cable based on Wright’s law²⁰. Our approach assumes that the unit costs of PV and wind power will decline as the cumulative capacity increases over time. We then estimate the fraction of reduction in the unit cost of PV and wind power based on the accumulation of the installed PV or wind-power capacity by country⁹¹:

$$\sigma_x = 1 - \left(\max \left(\frac{\sum_{y=1}^x P_y + P_{e,z,0}}{\max(P_{e,z,0}, P_{China,z,0})}, 1 \right) \right)^{\log_2(1-r_z)}, \quad x, y \in \epsilon \quad (7)$$

where ϵ is a country (1 to 192), x is a PV or wind plant in a country ϵ , σ_x is the fraction of cost reduction due to technological improvements when building a plant x , y is a PV or wind plant built before the power plant x in a country ϵ , z is a type of renewables (PV or wind power), P_y is the capacity of the power plant y , $P_{e,z,0}$ is the capacity built by 2020 in a country ϵ , and r_z is the rate of learning. We notice that the predicted σ_x would be unreasonably high when adopting an extremely low $P_{e,z,0}$ in countries with a low share of PV or wind energy in total power supply in 2020 because these countries are likely adopting technologies from other countries (e.g., China with the largest production of PV and wind power in 2020¹⁸). To determine the initial condition of technological improvements, we assume that the effects of learning on cost reduction for PV and wind power start in a country when the cumulative capacity of PV or wind power reaches China’s capacity in 2020²⁷.

We consider the effects of technological improvements in cost reduction when deploying CCS and low-carbon energy other than PV and wind power (bioenergy, geothermal, hydro, nuclear, and tidal wave) at a global scale due to a lack of national data for these technologies. We predict the fraction of cost reduction for these technologies based on the accumulation of the global capacity of CCS and low-carbon energy other than PV and wind power⁹¹:

$$\sigma_t = 1 - \left(\frac{P_{z,t} + P_{z,0}}{P_{z,0}} \right)^{\log_2(1-r_z)} \quad (8)$$

where z is CCS or a type of low-carbon energy other than PV or wind power (i.e. $z=1-6$ for bioenergy, geothermal, hydro, nuclear, tidal wave, and CCS, respectively), t is a year, $P_{z,0}$ is the total capacity of a low-carbon energy z built by 2020 (879.6 and 5171.9 TWh y⁻¹ for CCS and other types of low-carbon energy, respectively), $P_{z,t}$ is the capacity of a low-carbon energy z that has been built since 2021, and r_z is the learning rate for a low-carbon energy z . We adopt the average rates of learning for PV panels (25.9±13.5% for developing countries and 18±10.8% for

developed countries), wind turbines (12.2±3.6% for developing countries and 7.3±2.5% for developed countries), CCS (3.2%) and other types of low-carbon energy (5.1%) based on the time series of low-carbon energy prices observed in 26 countries over the period of 1981–2020 (Supplementary Table 10). Renewables have been rapidly developed worldwide in the past decade. Way et al.²⁰ has proven that the costs of renewables could be overestimated by energy-economy models if the rates of learning are underestimated. This method has been adopted by energy system models^{21,91–93}. In our model, we have used the method recommended by Way et al.²⁰ to predict the effects of technological learning by adopting the average rates of learning from measurements, allowing us to capture the potential impacts of technological changes on the deployment of PV and wind power. However, the rates of learning adopted in our study do not indicate that the prices of renewables will decrease greatly in the future. For example, assuming that the rate of learning is 20%, the cost will decrease by 77.3% when the capacity increases from 0.1 GW to 10 GW, but the cost will decrease merely by 19.9% when the capacity increases from 10 GW to 20 GW. Our model has accounted for the fact that there is a decreasing potential to further reduce the cost of renewables.

Regional supply chains of photovoltaic panels and wind turbines

We predict the fraction of reduction in the costs of deploying PV and wind power in each country by considering the establishment of regional or global supply chains to achieve the minimal prices of PV panels, wind turbines, mounting materials, secondary equipments, inverters, transformers, cables, and grid connection across 192 countries. We predict the fraction of cost reduction due to the supply chain by comparing the prices between countries:

$$\varphi_{x,Q} = 1 - \left(\frac{\min_{\epsilon}(\delta_{\epsilon,Q,t})}{\delta_{y,Q,t}} \right) \quad (9)$$

where x is a PV or wind power plant, ϵ is a country, φ_x is the fraction of cost reduction when building a plant x , Q is a cost component that will be covered by the regional or global supply chains (i.e. $Q=1-8$ for PV panels, wind turbines, mounting materials, secondary equipments, inverters, transformers, cables, and grid connection, respectively), t is the year when building a plant x , $\delta_{\epsilon,Q,t}$ is the price of a component Q in a country ϵ in a year t , and y is the country where a new plant x is built.

Global trade of minerals

We consider the supply of minerals as a limiting factor, which constrains the rate of growth in the capacities of PV and wind power in a country⁹⁴. We consider the consumption of copper (Cu), silicon (Si), zinc (Zn), and nickel (Ni) in the production of PV panels and the consumption of Cu, Zn, Ni, manganese (Mn), chromium (Cr) and rare-earth elements (REEs) in the production of wind turbines. We estimate the supply of minerals by compiling the national reserves and annual production of Si, Cu, Zn, Ni, Mn, Cr, and REEs in 43 countries from the Global Mineral Database that is developed by the U.S. Geological Survey⁷⁷. For the remaining countries, we disaggregate the annual production of Si, Cu, Zn, Ni, Mn, Cr, and REEs in other regions of the World given by the U.S. Geological Survey⁷⁷ to each country using the national territorial area as a proxy, which leads to annual productions of 2.5 kg Si, 40.4 kg Cu, 28.3 kg Zn, 5.8 kg Ni, 2.6 kg Mn, 32.2 kg Cr, and 0.004 kg REEs per squared kilometer. When building a new PV or wind-power plant in a country, we consider that the consumption of each mineral cannot exceed the supply, which is derived as the sum of production and import minus export. We consider that minerals produced by each country is firstly used to meet the demand in this country before export. The surplus of minerals will be exported to a country with a PV or wind-power plant that has been identified with the lowest LCOE.

Impacts of energy transitions on job creation and unemployment

We consider the impacts of energy transitions on employment, including project planning, manufacture and procurement, transportation, installation and grid connection, fuel supply, operation, maintenance, and decommissioning^{95,96}. We take into account the changes in employment in the transitions from coal, gas, and oil to various types of low-carbon energy including PV, onshore wind, offshore wind, bioenergy, geothermal, hydro, nuclear, and tidal wave. We also account for employment when expanding the capacities of power transmission and energy storage. Considering the effects of technological advances in reducing the hours of labor⁹⁷ and the employment factor⁹⁶, we predict the change in the direct, indirect, and induced employment in the power sector based on the targets of CO₂ emissions reduction:

$$EM_{p,t} = \sum_{z=1}^{11} (EMI_{z,t} + EMO_{z,t} + EMF_{z,t}) + EM_{s,t} + EM_{tr,t} \quad (10)$$

$$EMI_{z,t} = \sum_{d=1}^3 (I_{d,z,t_0} \cdot (1 - DF_z)^{t-t_0} \cdot (1 + CW_z)^{t-t_0} \cdot (P_{z,t} - P_{z,t-1})) \quad (11)$$

$$EMO_{z,t} = \sum_{d=1}^3 (O_{d,z,t_0} \cdot (1 - DF_z)^{t-t_0} \cdot (1 + CW_z)^{t-t_0} \cdot P_{z,t}) \quad (12)$$

$$EMF_{z,t} = FS_{z,t_0} \cdot (1 - DF_z)^{t-t_0} \cdot (1 + CW_z)^{t-t_0} \cdot EfS_{z,t} \quad (13)$$

$$EM_{s,t} = \sum_{n=1}^{sn} \left[\sum_{d=1}^3 (I_{d,s,t_0} \cdot (1 - DF_s)^{t-t_0} \cdot (1 + CW_s)^{t-t_0} \cdot \max(\Lambda_{s,h,n})) \right] \quad (14)$$

$$EM_{tr,t} = \sum_{l=1}^{n_l} \left[\sum_{d=1}^3 (I_{d,tr,t_0} \cdot (1 - DF_{tr})^{t-t_0} \cdot (1 + CW_{tr})^{t-t_0} \cdot D_l \cdot P_{UHV} \cdot \text{int} \left(\frac{\max \omega_{l,h}}{P_{UHV}} \right) \right] \quad (15)$$

where t is the year (t_0 is the first year), z is the type of power generation (1–11 for coal, gas, oil, PV, onshore wind, offshore wind, bioenergy, geothermal, hydro, nuclear, and tidal wave, respectively), s is the type of energy storage (1–3 for hydro pump, chemical batteries, and electric vehicles, respectively), tr is the type of UHV line (1–3 for ± 800 kV DC, ± 1100 kV DC, and 1000 kV AC, respectively), d is the type of employment (1–3 for direct, indirect and induced employment factor, respectively), n is a station for energy storage, s_n is the total number of stations for energy storage, l is a UHV line, n_l is the total number of UHV lines, $EM_{p,t}$ is the total number of workers in the power sector in a year, $EMI_{z,t}$ is the total number of workers involved in the construction for a type of power generation, $EMO_{z,t}$ is the total number of workers involved in the operation and maintenance for a type of power generation, $EMF_{z,t}$ is the total number of workers involved in the fuel supply for a type of power generation, $EM_{s,t}$ is the total number of workers involved in a type of energy storage, $EM_{tr,t}$ is the total number of workers involved in a type of power transmission, I_{d,z,t_0} is the initial employment factor for the construction of a type of power generation, DF_z is the rate of decrease in the employment factor, CW_z is the rate of change in the labor time for a worker in the power-generation sector, $P_{z,t}$ is the capacity of one type of power generation, O_{d,z,t_0} is the initial employment factor for the operation and maintenance of a type of power generation, FS_{z,t_0} is the initial employment factor for fuel supply, $EfS_{z,t}$ is the amount of fuel supply, I_{d,s,t_0} is the initial

employment factor for energy storage, DF_s is the rate of decrease in the employment factor of energy storage, CW_s is the rate of change in the labor time for a worker in the energy-storage sector, $\Lambda_{s,h,n}$ is the hourly energy storage in the station n , I_{d,tr,t_0} is the initial employment factor for power transmission, DF_{tr} is the rate of decrease in the employment factor of power transmission, CW_{tr} is the rate of change in the labor time for a worker in the power-transmission sector, D_l is the length of a UHV line, $\omega_{l,h}$ is the hourly transmission of electricity, P_{UHV} is the capacity designed for a UHV line (8 or 12 GW for a DC line or 3 to 6 GW for an AC line). All parameters used in the calculation are listed in Supplementary Data 6.

Biodiversity loss due to installation of photovoltaic panels and wind turbines

We estimate the fraction of biodiversity loss due to the installation of PV panels and wind turbines (L_i) at a spatial resolution of 0.0083° in latitude and 0.033° in longitude using the method developed by Kehoe et al.⁹⁸ and Xiong et al.⁹⁹:

$$L_i = 1 - \frac{S_{PW}}{S_{x(i)}} \quad (16)$$

where i is a pixel, $x(i)$ is the type of land use in the pixel (i.e., 1 to 10 for closed shrubland, open shrubland, woody savanna, savanna, grassland, croplands, vegetation mosaics, snow and ice, desert, and water bodies, respectively), S_x is the richness of species in terms of land use^{98,99}, and S_{PW} is the richness of species for the land installed with PV panels or wind turbines (50)⁹⁸. We estimate the fraction of biodiversity loss in each country based on the fraction of biodiversity loss due to the installation of PV panels and wind turbines and the spatial distribution of species richness at a spatial resolution of 1° in latitude and 1° in longitude⁹⁹.

Marginal abatement costs

We estimate the marginal abatement costs of PV and wind power at a plant level based on the optimized capacities and construction period of each PV or wind-power plant. When building a new PV or wind power plant, we predict the marginal abatement costs ($\xi_{\epsilon,t,\vartheta}$) based on the marginal changes in total costs when deploying PV and wind power, reduction of total CO₂ emissions by replacing fossil fuels, change in the revenue from replacing fossil fuels, and additional CO₂ emissions due to land-use change:

$$\xi_{\epsilon,t,\vartheta} = \frac{E_{\vartheta} \cdot M_{\vartheta} - E_{\vartheta-1} \cdot M_{\vartheta-1} - p_{ff} \cdot (E_{\vartheta} - E_{\vartheta-1})}{F_{\epsilon,t,\vartheta-1} - F_{\epsilon,t,\vartheta}} \quad (17)$$

$$F_{\epsilon,t,\vartheta} = e_{ff} \cdot (\Gamma_{\epsilon,t} - E_{\vartheta}) + \sum_{x=1}^{\vartheta} \sum_{n=1}^{N_x} (FS_n \cdot A_n) + \frac{\sum_{n=1}^{n_{\vartheta}} (CS_n \cdot A_n)}{T_f} \quad (18)$$

where ϵ is a country ($\epsilon=1$ to 192), ϑ is a new PV or wind plant in a country ϵ , t is the year building a plant ϑ , E_{ϑ} is total power generation by low-carbon energy after building a plant ϑ , M_{ϑ} is the LCOE of PV and wind power when building a plant ϑ , $F_{\epsilon,t,\vartheta}$ is total CO₂ emissions from fossil fuels when building a plant ϑ , $\Gamma_{\epsilon,t}$ is the total demand for power in a year t in a country ϵ , p_{ff} is the unit cost of fossil fuels when generating one kilowatt-hour of electricity, e_{ff} is the average CO₂ emission factor of fossil fuels in each country, x is a PV or wind plant built before a plant ϑ , n is a pixel, N_x is the number of pixels covered by a plant x , FS_n is the flux of terrestrial carbon sink in a pixel n ¹⁰⁰, CS_n is the content of carbon in soils in the pixel n ¹⁰¹, A_n is the total area of a pixel n , and T_f is the average lifetime of a PV or wind-power plant (25 years)⁸⁸. We consider that the electricity generated by low-carbon energy can be used to replace oil, gas, and coal in the order of their prices for profit maximization, where the composition of fossil fuels is determined by

country using the historical data in 2020¹⁰². We estimate the unit cost of fossil fuels when generating one kilowatt-hour of electricity (p_{ff}) based on the mass-based prices of coal, oil, and gas (Supplementary Data 1), the calorific values of coal, oil, and gas (Supplementary Data 2), and the efficiency of power generation (35% for coal, 38% for oil, and 45% for gas)¹⁰³. We estimate the average CO₂ emission factor of fossil fuels (e_{ff}) based on the CO₂ emission factors of coal, oil, and gas in 30 countries (Supplementary Data 3) and the composition of fossil fuels by country in 2020¹⁰².

Data availability

Data used for our analyses are available on the GitHub repository: <https://github.com/rongwang-fudan/global-PV-wind>. Preprocessed outputs are available at: <https://zenodo.org/records/14736435>. Global hourly direct and diffuse solar radiation, air temperature, friction velocity, zero-plane displacement height, and length of roughness can be accessed from MERRA-2 (<https://disc.gsfc.nasa.gov/datasets>). Future power demand, power generation of PV, onshore wind, offshore wind, bioenergy, geothermal, hydro, nuclear, and tidal wave, and investment for power transmission and storage are available from the International Institute for Applied Systems Analysis (IIASA; <https://data.ece.iiasa.ac.at/ar6/>). Material production and reserve of copper, zinc, nickel, silicon, manganese, chromium, and rare-earth elements by country are compiled from the United States Geological Survey Global Mineral Database (<https://www.usgs.gov/centers/national-minerals-information-center/commodity-statistics-and-information>). Source data are provided in this paper.

Code availability

The model is implemented in the open-source framework MATLAB. The code used in this paper are available on the open repository <https://github.com/rongwang-fudan/global-PV-wind>, and the version used to generate the results presented here is available via Zenodo (<https://zenodo.org/records/14736435>)¹⁰⁴.

References

- Tollefson, J. Is it too late to keep global warming below 1.5 °C? The challenge in 7 charts. *Nature*. <https://www.nature.com/immersive/d41586-023-03601-6/index.html> (2023).
- Matthews, H. & Wynes, S. Current global efforts are insufficient to limit warming to 1.5 °C. *Science* **376**, 1404–1409 (2022).
- Burke, M., Davis, W. & Diffenbaugh, N. Large potential reduction in economic damages under UN mitigation targets. *Nature* **557**, 549 (2018).
- Armstrong McKay, D. et al. Exceeding 1.5°C global warming could trigger multiple climate tipping points. *Science* **377**, 6611 (2022).
- Intergovernmental Panel on Climate Change. Climate Change 2022: Mitigation of Climate Change. <https://www.ipcc.ch/report/ar6/wg3/> (IPCC, 2022).
- Meinshausen, M. et al. Realization of Paris Agreement pledges may limit warming just below 2 °C. *Nature* **604**, 304–309 (2022).
- WMO. Climate change indicators reached record levels in 2023: WMO. <https://wmo.int/media/news/climate-change-indicators-reached-record-levels-2023-wmo> (2024).
- WMO. WMO confirms 2024 as warmest year on record at about 1.55 °C above pre-industrial level. <https://wmo.int/news/media-centre/wmo-confirms-2024-warmest-year-record-about-155degc-above-pre-industrial-level> (2025).
- Jones, N. When will global warming actually hit the landmark 1.5 °C limit? *Nature* **618**, 20 (2023).
- Intergovernmental Panel on Climate Change. Global Warming of 1.5 °C. <https://www.ipcc.ch/sr15/> (IPCC, 2018).
- Intergovernmental Panel on Climate Change. Climate Change 2021: The Physical Science Basis <https://www.ipcc.ch/report/ar6/wg1/> (IPCC, 2021).
- Creutzig, F. et al. Considering sustainability thresholds for BECCS in IPCC and biodiversity assessments. *Glob. Change Biol. Bioenergy* **13**, 510–515 (2021).
- Tong, D. et al. Committed emissions from existing energy infrastructure jeopardize 1.5°C climate target. *Nature* **572**, 373–377 (2019).
- UN Environment Programme (UNEP). Emissions Gap Report 2023. <https://www.unep.org/resources/emissions-gap-report-2023> (2023).
- Sanderson, K. COP28 climate summit signals the end of fossil fuels—but is it enough? *Nature* **624**, 624 (2023).
- Edward, B. et al. AR6 Scenarios Database hosted by IIASA. <https://data.ece.iiasa.ac.at/ar6/> (International Institute for Applied Systems Analysis, 2022).
- U. S. Energy Information Administration. International Electricity Database. <https://www.eia.gov/international/data/world> (2022).
- Cherp, A. et al. National growth dynamics of wind and solar power compared to the growth required for global climate targets. *Nat. Energy* **6**, 742–754 (2021).
- International Energy Agency. World Energy Outlook 2022. <https://www.iea.org/reports/world-energy-outlook-2022> (International Energy Agency, Paris, France, 2022).
- Way, R. et al. Empirically grounded technology forecasts and the energy transition. *Joule* **6**, 2057–2082 (2022).
- Nijse, F. J. M. M. et al. The momentum of the solar energy transition. *Nat. Commun.* **14**, 6542 (2023).
- Creutzig, F., Hilaire, J., Nemet, G., Müller-Hansen, F. & Minx, J. C. Technological innovation enables low cost climate change mitigation. *Energy Res. Soc. Sci.* **105**, 103276 (2023).
- Wang, Y. et al. Accelerating the energy transition towards photovoltaic and wind in China. *Nature* **619**, 761–767 (2023).
- Jerez, S. et al. Future changes, or lack thereof, in the temporal variability of the combined wind-plus-solar power production in Europe. *Renew. Energ.* **139**, 251–260 (2019).
- Harrison-Atlas, D. et al. Temporal complementarity and value of wind-PV hybrid systems across the United States. *Renew. Energ.* **201**, 111–123 (2022).
- Giurco, D. et al. *Achieving Paris Climate Agreement Goals* (Springer Cham, 2019).
- Helveston, J., He, G. & Davidson, M. Quantifying the cost savings of global solar photovoltaic supply chains. *Nature* **612**, 83–87 (2022).
- International Renewable Energy Agency. Renewable power generation costs in 2021 (IREA, 2022).
- Denholm, P. et al. Land Use Requirements of Modern Wind Power Plants in the United States. <https://doi.org/10.2172/964608> (2009).
- Chen, Y., Kirkerud, J. G. & Bolkesjø, T. F. Balancing GHG mitigation and land-use conflicts: Alternative Northern European energy system scenarios. *Appl. Energ.* **310**, 118557 (2022).
- United States Geological Survey. Land cover type yearly L3 global 500 m SIN grid. <https://lpdaac.usgs.gov/products/mcd12q1v006/> (2014).
- Luo, Y. et al. Hybrid Global Annual 1-km IGBP Land Cover Maps for the Period 2000–2020. *J. Remote Sens.* **4**, 0122 (2024).
- McKinsey & Company. Pathways to a Low-Carbon Economy: Version 2 of the Global Greenhouse Gas Abatement Cost Curve https://www.mckinsey.com/-/media/mckinsey/dotcom/client_service/sustainability/cost%20curve%20pdfs/pathways_lowcarbon_economy_version2.ashx (McKinsey&Company, 2009).
- Davidson, M. R. et al. Modelling the potential for wind energy integration on China's coal-heavy electricity grid. *Nat. Energy* **1**, 1–7 (2016).
- Eberhard, A. et al. Accelerating investments in power in sub-Saharan Africa. *Nat. Energy* **2**, 1–5 (2017).

36. Lu, T. et al. India's potential for integrating solar and on-and off-shore wind power into its energy system. *Nat. Commun.* **11**, 1–10 (2020).
37. Zhang, D. et al. Spatially resolved land and grid model of carbon neutrality in China. *Proc. Natl. Acad. Sci. USA* **121**, e2306517121 (2024).
38. IRENA. Electricity statistics (MW/GWh) by Country/area, Technology, Data Type, Grid connection and Year. https://pxweb.irena.org/pxweb/en/IRENASTAT/IRENASTAT_Power%20Capacity%20and%20Generation/Country_ELECSTAT_2024_H2.px/ (2024).
39. IEA. Batteries and Secure Energy Transitions. <https://iea.blob.core.windows.net/assets/cb39c1bf-d2b3-446d-8c35-aae6b1f3a4a0/BatteriesandSecureEnergyTransitions.pdf> (2024).
40. IEA. Net Zero by 2050: A Roadmap for the Global Energy Sector. https://iea.blob.core.windows.net/assets/deebef5d-0c34-4539-9d0c-10b13d840027/NetZeroBy2050-ARoadmapfortheGlobalEnergySector_CORR.pdf (2021).
41. World Integrated Trade Solution. National Minerals Information Center: Commodity Statistics and Information. <https://wits.worldbank.org/trade/comtrade/en/country/ALL/year/2021/tradeflow/Imports/partner/WLD/product/260200> (2024).
42. Tong, D. et al. Geophysical constraints on the reliability of solar and wind power worldwide. *Nat. Commun.* **12**, 6146 (2021).
43. GWEC. The Global Wind Energy Council at COP28. <https://gwec.net/cop28/> (2023).
44. IRENA. FUTURE OF WIND: Deployment, investment, technology, grid integration and socio-economic aspects. https://www.irena.org/-/media/Files/IRENA/Agency/Publication/2019/Oct/IRENA_Future_of_wind_2019.pdf?rev=c324896ba0f74c99a0cde784f3a36dff (2019).
45. IRENA. GLOBAL ENERGY TRANSFORMATION: A ROADMAP TO 2050. https://www.irena.org/-/media/Files/IRENA/Agency/Publication/2018/Apr/IRENA_Report_GET_2018.pdf (2018).
46. Buljan, A. Offshore Wind Could Grow 56-Fold by 2050 and Significantly Contribute to Green Hydrogen Production, DNV's New Report Says. <https://www.offshorewind.biz/2022/10/13/offshore-wind-could-grow-56-fold-by-2050-contribute-to-green-hydrogen-production/> (2022).
47. IEA. Global renewable energy capacity by scenario, 2022 and 2030. <https://www.iea.org/data-and-statistics/charts/global-renewable-energy-capacity-by-scenario-2022-and-2030> (2024).
48. IEA. Global installed energy storage capacity by scenario, 2023 and 2030. <https://www.iea.org/data-and-statistics/charts/global-installed-energy-storage-capacity-by-scenario-2023-and-2030> (2024).
49. Aghahosseini, A. et al. Energy system transition pathways to meet the global electricity demand for ambitious climate targets and cost competitiveness. *Appl. Energy* **331**, 120401 (2023).
50. Haegel, N. M. et al. Terawatt-scale photovoltaics: Transform global energy. *Science* **364**, 836–838 (2019).
51. DNV. ENERGY TRANSITION OUTLOOK 2023. <https://www.dnv.com/publications/energy-transition-outlook-2023-247935> (2023).
52. Wang, S. et al. Future demand for electricity generation materials under different climate mitigation scenarios. *Joule* **7**, 309–332 (2023).
53. Gaucher, Y. et al. Limited impact of COVID-19 recovery packages on near-term CO₂ emissions pathways. *Environ. Res. Commun.* **4**, 101006 (2022).
54. Climate Policy Initiative (CPI). Global Landscape of Climate Finance 2023. <https://www.climatepolicyinitiative.org/publication/global-landscape-of-climate-finance-2023/> (2023).
55. Bloomberg. Energy Transition Investment Trends 2024. <https://about.bnef.com/energy-transition-investment/> (2024).
56. Turney, D. & Fthenakis, V. Environmental impacts from the installation and operation of large-scale solar power plants. *Renew. Sust. Energy. Rev.* **15**, 3261–3270 (2011).
57. Rahman, A., Farrok, O. & Haque, M. M. Environmental impact of renewable energy source based electrical power plants: Solar, wind, hydroelectric, biomass, geothermal, tidal, ocean, and osmotic. *Renew. Sust. Energy. Rev.* **161**, 112279 (2022).
58. Xie, J. J., Martin, M., Rogelj, J. & Staffell, I. Distributional labour challenges and opportunities for decarbonizing the US power system. *Nat. Clim. Change* **13**, 1203–1212 (2023).
59. Carley, S. & Konisky, D. M. The justice and equity implications of the clean energy transition. *Nat. Energy* **5**, 569–577 (2020).
60. Lim, J., Aklin, M. & Frank, M. R. Location is a major barrier for transferring US fossil fuel employment to green jobs. *Nat. Commun.* **14**, 5711 (2023).
61. Patel, R. Underwater HVDC-based Grid: Pushing the Limits of Power Transmission. <https://www.allaboutcircuits.com/news/underwater-HVSC-based-grid-pushing-the-limits-of-power-transmission/> (2021).
62. Žuk, P. & Žuk, P. National energy security or acceleration of transition? Energy policy after the war in Ukraine. *Joule* **6**, 709–712 (2022).
63. Fu, R. et al. Tracing metal footprints via global renewable power value chains. *Nat. Commun.* **14**, 3703 (2023).
64. Veers, P. et al. Grand challenges in the science of wind energy. *Science* **366**, eaau2027 (2019).
65. Mach, K. J. et al. Climate as a risk factor for armed conflict. *Nature* **571**, 193–197 (2019).
66. Kleimann, D. et al. How Europe Should Answer the US Inflation Reduction Act. Bruegel. JSTOR <https://www.jstor.org/stable/resrep48672> (2023).
67. Masters, M. *Renewable and Efficient Electric Power Systems* (John Wiley & Sons, 2013).
68. Chen, S. et al. The potential of photovoltaics to power the belt and road initiative. *Joule* **3**, 1895–1912 (2019).
69. Rinne, E., Holttinen, H., Kiviluoma, J. & Rissanen, S. Effects of turbine technology and land use on wind power resource potential. *Nat. Energy* **3**, 494–500 (2018).
70. Global Modeling and Assimilation Office. GEOS Atmospheric Assimilation Products, National Aeronautics and Space Administration. https://gmao.gsfc.nasa.gov/GMAO_products/NRT_products.php (2021).
71. Global Administrative Areas data. Administrative areas of all countries https://gadm.org/download_world.html (2022).
72. Resource and Environment Science and Data Center. Environmental Protection Areas. <https://www.resdc.cn/data.aspx?DATAID=137> (2020).
73. United States Geological Survey. Shuttle radar topography mission. <https://earthexplorer.usgs.gov/> (2015).
74. Flanders Marine Institute. Maritime boundaries geodatabase: Maritime boundaries and exclusive economic zones (200NM), version 10, Maritime Boundaries Geodatabase. <http://www.vliz.be/en/imis?dasid=5465&doid=312> (2018).
75. UN Environment Programme World Conservation Monitoring Centre. Protected Area Profile for China from the World Database of Protected Areas www.protectedplanet.net/ (2021).
76. U.S. Energy Information Administration. Hourly electric grid monitor <https://www.eia.gov/electricity/gridmonitor/dashboard/custom/pending> (2022).
77. Kumm, M. et al. Gridded global datasets for Gross Domestic Product and Human Development Index over 1990–2015. *Sci. Data* **5**, 180004 (2018).
78. National Development and Reform Commission. Typical Power load curves of provincial power networks in China <http://www.>

- gov.cn/xinwen/2019-12/30/content_5465088.htm (National Development and Reform Commission, China, 2019).
79. Brinkerink, M. & Deane, P. PLEXOS-World 2015, Harvard Dataverse <https://doi.org/10.7910/DVN/CBYXBY> (2021).
 80. U.S. Geological Survey. Commodity Statistics and Information–NONFUEL MINERALS <https://www.usgs.gov/centers/national-minerals-information-center/commodity-statistics-and-information> (2023).
 81. Chen, X. et al. Pathway toward carbon-neutral electrical systems in China by mid-century with negative CO₂ abatement costs informed by high-resolution modeling. *Joule* **5**, 2715–2741 (2021).
 82. Cole, W. & Frazier, A. *Cost Projections for Utility-Scale Battery Storage* (National Renewable Energy Lab, Golden, CO, United States, 2019).
 83. Stocks, M. et al. Global atlas of closed-loop pumped hydro energy storage. *Joule* **5**, 270–284 (2021).
 84. Mingle, J. Does the path to a low-carbon future run through a global grid? <https://chinaproject.harvard.edu/news/commentary-global-grid> (2018).
 85. Renewable Energy Institute. Connecting Renewables to the Global Energy Grid <https://www.renewable-ei.org/en/asg/> (REI, 2019).
 86. Yan, J., Yang, Y., Campana, P. & He, J. City-level analysis of subsidy-free solar photovoltaic electricity price, profits and grid parity in China. *Nat. Energy* **4**, 709–717 (2019).
 87. Xiang, C., Chen, F., Wen, F. & Song, F. Can China's offshore wind power achieve grid parity in time? *Int. J. Green Energy* **18**, 1219–1228 (2021).
 88. Victoria, M. et al. Solar photovoltaics is ready to power a sustainable future. *Joule* **6**, 1041–1056 (2021).
 89. International Energy Agency. GHG abatement costs for selected measures of the Sustainable Recovery Plan <https://www.iea.org/data-and-statistics/charts/ghg-abatement-costs-for-selected-measures-of-the-sustainable-recovery-plan> (IEA, 2022).
 90. Crawford, I. & Howland, M. Why don't we use tidal power more?, Climate Portal <https://climate.mit.edu/ask-mit/why-dont-we-use-tidal-power-more?> (2022).
 91. McDonald, A. & Schrattenholzer, L. Learning rates for energy technologies. *Energy Polic.* **29**, 255–261 (2001).
 92. Achakulwisut, P. et al. Global fossil fuel reduction pathways under different climate mitigation strategies and ambitions. *Nat. Commun.* **14**, 5425 (2023).
 93. Davis, S. J. et al. Emissions rebound from the COVID-19 pandemic. *Nat. Clim. Change* **12**, 412–414 (2022).
 94. International Energy Agency. The Role of Critical Minerals in Clean Energy Transitions <https://www.iea.org/reports/the-role-of-critical-minerals-in-clean-energy-transitions> (IEA, 2021).
 95. IRENA. Renewable Energy Benefits Leveraging Local Capacity for Solar PV. https://www.irena.org/-/media/Files/IRENA/Agency/Publication/2017/Jun/IRENA_Leveraging_for_Solar_PV_2017.pdf (2017).
 96. Rutovitz, J. *Calculating Global Energy Sector Jobs 2015 Methodology*. (University of Technology Sydney, 2015).
 97. Sasse, J. P. & Trutnevyte, E. A low-carbon electricity sector in Europe risks sustaining regional inequalities in benefits and vulnerabilities. *Nat. Commun.* **14**, 2205 (2023).
 98. Kehoe, L. et al. Biodiversity at risk under future cropland expansion and intensification. *Nat. Ecol. Evol.* **1**, 1129–1135 (2017).
 99. Xiong, Y. et al. Potential impacts of pandemics on global warming, agricultural production, and biodiversity loss. *One Earth* **7**, 697–713 (2024).
 100. Wang, H. et al. Global terrestrial ecosystem carbon flux inferred from TanSat XCO₂ retrievals. *J. Remote. Sens.* **2022**, <https://doi.org/10.34133/2022/9816536> (2022).
 101. Spawn, S. et al. Harmonized global maps of above and below-ground biomass carbon density in the year 2010. *Sci. Data* **7**, 112 (2020).
 102. Ember. Electricity Data Explorer <https://ember-climate.org/data/data-tools/data-explorer/> (Sandbag Climate Campaign CIC, 2023).
 103. Zeiss, G. Energy Efficiency of Fossil Fuel Power Generation <https://geospatial.blogs.com/geospatial/2010/01/energy-efficiency-of-fossil-fuel-power-generation.html> (2010).
 104. Wang, R. rongwang-fudan/global-PV-wind: Global spatiotemporal optimization of photovoltaic and wind power to achieve the Paris Agreement targets (v1.0.0). Zenodo. <https://doi.org/10.5281/zenodo.14736435> (2025).

Acknowledgements

We thank F. E. Benth, L.B. Wu, and X.Y. Zhang for the useful discussion. This study is funded by the National Key R&D Program of China (No. 2022YFF0802504) and the National Natural Science Foundation of China (No. 41877506 and 42341205). R.W., J.M.C., X.T., and R.H.Z. acknowledge support from the Shanghai International Science and Technology Partnership Project (No. 21230780200), and the Shanghai B&R Joint Laboratory Project (No. 22230750300). Y.J.W. acknowledges support from the Shanghai Tongji Gaotingyao Environmental Science & Technology Development Foundation. K.T. benefits from state assistance managed by the National Research Agency in France under the Program d'Investissements d'Avenir under the reference ANR-19-MPGA-0008. P.C. acknowledges support from the ANR CLAND Convergence Institute 16-CONV-0003. J.P. and J.S. acknowledge the financial support from the Catalan Government grant SGR 2017–1005, the Spanish Government grants PID2019–110521GB-I00, PID2020–115770RB-I00, and TED2021–132627B-I00 funded by MCIN, AEI/10.13039/501100011033 funded by the European Union Next Generation EU/PRTR, and the Fundación Ramón Areces grant CIVP20A6621.

Author contributions

R.W. initiated the study, led the project, and designed the research. Y.J.W. compiled data, performed the research, and prepared graphs. K.T., P.C., J.P., Y.B., J.S., D.H., J.J.C., J.M.C., L.W., X.T., and R.H.Z. contributed to data analysis. R.W. wrote the first draft of the paper. R.W., Y.J.W., K.T., P.C., J.P., Y.B., J.S., D.H., J.J.C., J.M.C., L.W., X.T., and R.H.Z. critically revised successive drafts of the paper and approved the final version.

Competing interests

The authors declare no competing interests.

Additional information

Supplementary information The online version contains supplementary material available at <https://doi.org/10.1038/s41467-025-57292-w>.

Correspondence and requests for materials should be addressed to Rong Wang.

Peer review information *Nature Communications* thanks Qusay Hassan, Christian Calvillo Munoz, and the other anonymous reviewer(s) for their contribution to the peer review of this work. A peer review file is available.

Reprints and permissions information is available at <http://www.nature.com/reprints>

Publisher's note Springer Nature remains neutral with regard to jurisdictional claims in published maps and institutional affiliations.

Open Access This article is licensed under a Creative Commons Attribution-NonCommercial-NoDerivatives 4.0 International License, which permits any non-commercial use, sharing, distribution and reproduction in any medium or format, as long as you give appropriate credit to the original author(s) and the source, provide a link to the Creative Commons licence, and indicate if you modified the licensed material. You do not have permission under this licence to share adapted material derived from this article or parts of it. The images or other third party material in this article are included in the article's Creative Commons licence, unless indicated otherwise in a credit line to the material. If material is not included in the article's Creative Commons licence and your intended use is not permitted by statutory regulation or exceeds the permitted use, you will need to obtain permission directly from the copyright holder. To view a copy of this licence, visit <http://creativecommons.org/licenses/by-nc-nd/4.0/>.

© The Author(s) 2025